Grenzschichtfernerkundung: Bestimmung der Mischungsschichthöhe und anderer Grenzschicht-strukturen aus SODAR, RASS und Ceilometer

Stefan Emeis
stefan.emeis@kit.edu

INSTITUTE OF METEOROLOGY AND CLIMATE RESEARCH, Atmospheric Environmental Research

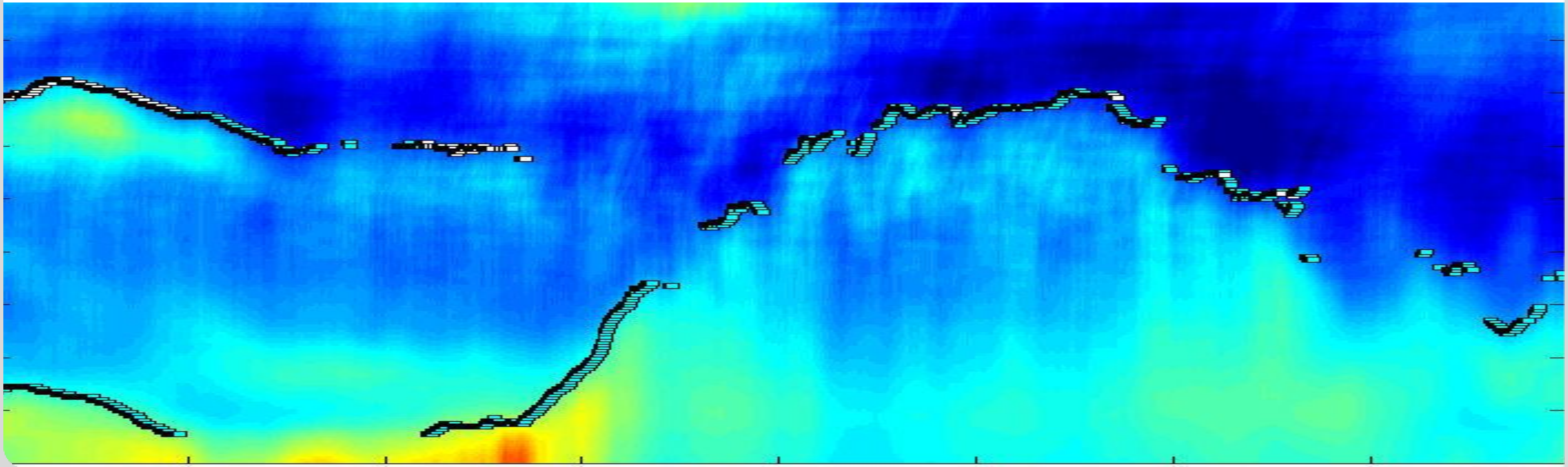

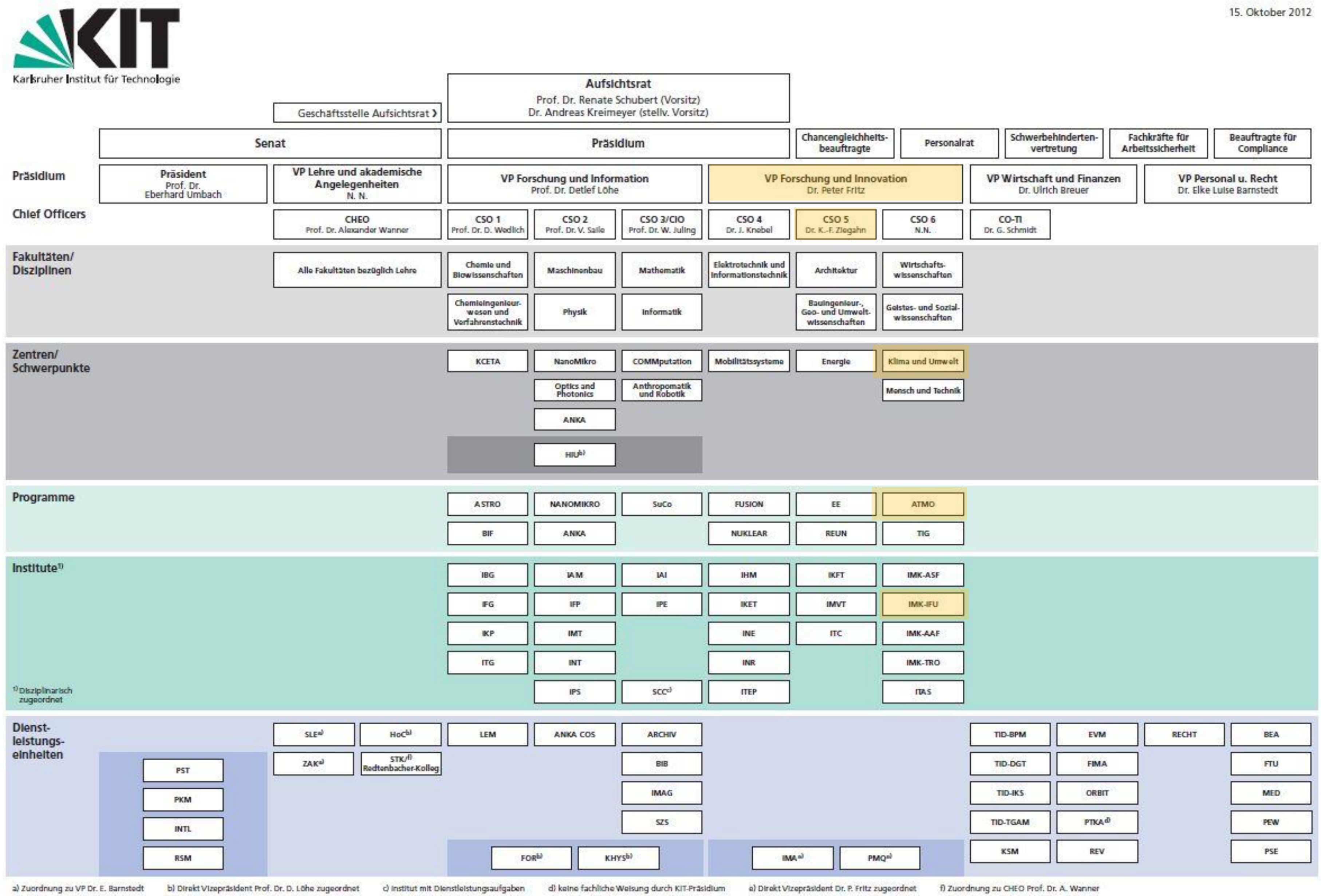
15. Oktober 2012
Karlsruher Institut für Technologie
Geschäftsstelle Aufsichtsrat
Aufsichtsrat
Prof. Dr. Renate Schubert (Vorsitz)
Dr. Andreas Kreimeyer (stellv. Vorsitz)
Senat
Präsidium
Chancengleichheits-beauftragte
Personalrat
Schwerbehinderten-vertretung
Fachkräfte für Arbeitssicherheit
Beauftragte für Compliance
Präsidium
Präsident Prof. Dr. Eberhard Umbach
VP Lehre und akademische Angelegenheiten N. N.
VP Forschung und Information Prof. Dr. Detlef Löhe
VP Forschung und Innovation Dr. Peter Fritz
VP Wirtschaft und Finanzen Dr. Ulrich Breuer
VP Personal u. Recht Dr. Elke Luise Barnstedt
Chief Officers
CHEO Prof. Dr. Alexander Wanner
CSO 1 Prof. Dr. D. Wedlich
CSO 2 Prof. Dr. V. Saile
CSO 3/CIO Prof. Dr. W. Juling
CSO 4 Dr. J. Knebel
CSO 5 Dr. K.-F. Ziegahn
CSO 6 N.N.
CO-TI Dr. G. Schmidt
Fakultäten/ Disziplinen
Alle Fakultäten bezüglich Lehre
Chemie und Biowissenschaften
Maschinenbau
Mathematik
Elektrotechnik und Informationstechnik
Architektur
Wirtschafts-wissenschaften
Chemieingenieur-wesen und Verfahrenstechnik
Physik
Informatik
Bauingenieur-, Geo- und Umwelt-wissenschaften
Geistes- und Sozial-wissenschaften
Zentren/ Schwerpunkte
KCETA
NanoMikro
COMMputation
Mobilitätssysteme
Energie
Klima und Umwelt
Optics and Photonics
Anthropomatik und Robotik
Mensch und Technik
ANKA
HIU b)
Programme
ASTRO
NANOMIKRO
SuCo
FUSION
EE
ATMO
BIF
ANKA
NUKLEAR
REUN
TIG
Institute 1)
IBG
IAM
IAI
IHM
IKFT
IMK-ASF
IFG
IFP
IPE
IKET
IMVT
IMK-IFU
IKP
IMT
INE
ITC
IMK-AAF
ITG
INT
INR
IMK-TRO
IPS
SCC c)
ITEP
ITAS
1) Disziplinarisch zugeordnet
Dienst-leistungs-einheiten
SLE a)
HoC b)
LEM
ANKA COS
ARCHIV
TID-BPM
EVM
RECHT
BEA
PST
ZAK a)
STK/f) Redtenbacher-Kolleg
BIB
TID-DGT
FIMA
FTU
PKM
IMAG
TID-IKS
ORBIT
MED
INTL
SZS
TID-TGAM
PTKA d)
PEW
RSM
FOR b)
KHYS b)
IMA e)
PMQ e)
KSM
REV
PSE
a) Zuordnung zu VP Dr. E. Barnstedt
b) Direkt Vizepräsident Prof. Dr. D. Löhe zugeordnet
c) Institut mit Dienstleistungsaufgaben
d) keine fachliche Weisung durch KIT-Präsidium
e) Direkt Vizepräsident Dr. P. Fritz zugeordnet
f) Zuordnung zu CHEO Prof. Dr. A. Wanner

October 2012

Institute of Meteorology and Climate Research (IMK-IFU)

Atmospheric Environmental Research

Head: Prof. Dr. Hans Peter Schmid
Deputy Head: Prof. Dr. Hans Papen

Kst. 5260

Specialist Officer at Establishment Level and Safety Officer:

Sifa	E. Langer
Sibe	St. Schmid
SSB	Prof. Dr. H. Papen
Laser	Dr. T. Trickl

Bio-Geo-Chemical Processes

Head: Prof. Dr. Klaus Butterbach-Bahl
Deputy Head: Prof. Dr. Hans Papen

- **Ecosystem Matter Fluxes**
  Dr. Ralf Kiese
- **Regionalization of Biogenic Trace Gas Fluxes**
  Prof. Dr. Klaus Butterbach-Bahl

Ecosystem-Atmosphere Interactions

Head: Prof. Dr. Almut Arneth
Deputy Head: Dr. Peter Werle

- **Plant-Atmosphere Interactions**
  Prof. Dr. Almut Arneth
- **Integrated Land-Atmosphere Surface-Exchange Research (iLASER)**
  Dr. Peter Werle
- **Transport Processes in the Atmospheric Boundary-Layer (TABLe), Helmholtz-Young Investigators Group**
  Dr. Matthias Mauder

Regional Climate Systems

Head: Prof. Dr. Harald Kunstmann
Deputy Head: Dr. Ralf Sussmann

- **Atmospheric Variability and Trends**
  Dr. Ralf Sussmann
- **Regional Coupling of Ecosystem-Atmosphere-Processes**
  Dr. Peter Suppan
- **Regional Climate and Hydrology**
  Prof. Dr. Harald Kunstmann

Ecological Observatory TERENO-prealpine

Prof. Dr. Hans Papen

World Calibration Center (WCC)

Dr. Rainer Steinbrecher

Helmholtz Research School MICMoR / Support of Young Scientists

Dr. B. Elija Bleher

Informationtechnology and Mechatronics

Head: Dipl.-Ing. Frank Neidl

Administration and Organization

Head: Prof. Dr. Hans Peter Schmid

IMK-IFU Personnel

- people with diverse training backgrounds and specializations
- supported by POF funding (~1/3) and externally funded research (~2/3)

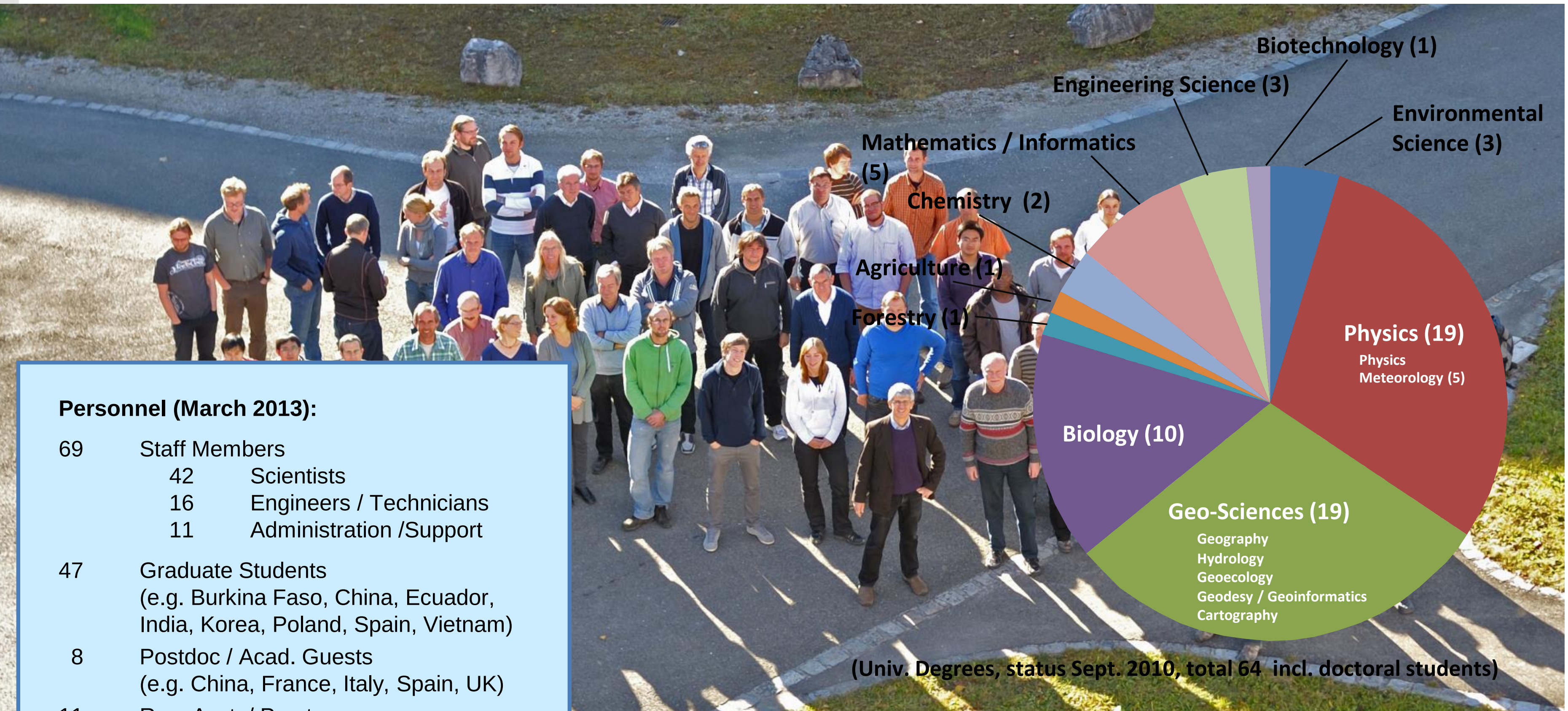

Personnel (March 2013):

69	Staff Members		
	42	Scientists	
	16	Engineers / Technicians	
	11	Administration /Support	
47	Graduate Students (e.g. Burkina Faso, China, Ecuador, India, Korea, Poland, Spain, Vietnam)		
8	Postdoc / Acad. Guests (e.g. China, France, Italy, Spain, UK)		
11	Res. Asst. / Pract.		
(135	Total)		

Remote sensing

of the vertical structure of the atmospheric boundary layer

WindForS Wind Energy Research Alliance

Basic remote sensing techniques

KIT Karlsruhe Institute of Technology

name	princple	spatial resolution	direction	type
RADAR	backscatter, electro-magnetic pulses, fixed wave length	profiling	scanning, slanted	active, monostatic
SODAR	backscatter, acoustic pulses, fixed wave length	profiling	fixed, slanted, vertical	active, usually monostatic
LIDAR ceilometer	backscatter, optical pulses, fixed wave length(s)	profiling	scanning, fixed, horizontal, slanted, vertical	active, monostatic
RASS	backscatter, acoustic, electro-magnetic, fixed wave length	profiling	fixed, vertical	active, monostatic
FTIR	absorption, infrared, spectrum	path-averaging	fixed, horizontal, slanted	active, bistatic or passive
FTIR	emission, infrared, spectrum	path-averaging	fixed, horizontal, slanted	passive
DOAS	absorption, optical, fixed wave lengths	path-averaging	fixed, horizontal	active, bistatic
radiometry	electro-magnetic, fixed wave length(s)	averaging, profiling	fixed, scanning, slanted, vertical	passive
tomography	travel time, acoustic, fixed wave length	horizontal distribution	fixed, horizontal	active, multiple emitters and receivers

subject of this lecture

subject of this lecture

Frequencies for atmospheric remote sensing

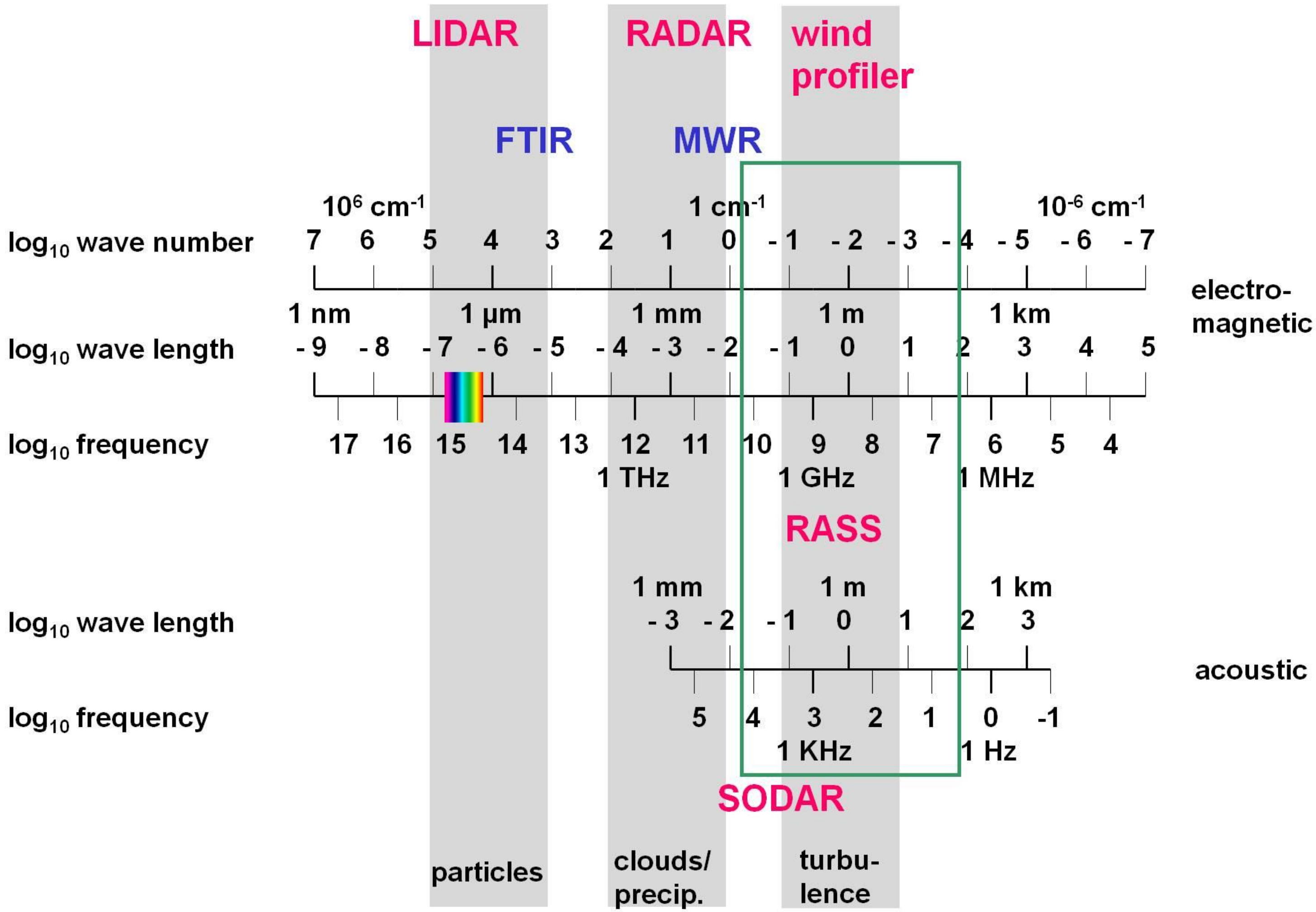

Emeis, S., 2010: Measurement Methods in Atmospheric Sciences - In situ and remote. Borntraeger, Stuttgart, 272 pp., 103 figs, 28 tables, ISBN 978-3-443-01066-9.

Surface-based Remote Sensing Systems

at IMK-IFU

SODAR (Large system), acoustic backscatter, Doppler shift analysis ➔ wind, turbulence

SODAR-RASS (Doppler-RASS), acoustic, electro-magnetic backscatter, determines speed of sound ➔ wind and temperature profiles

Ceilometer, backscatter, optical pulses, wave length ~ 0.9 µm ➔ aerosol profiles

Wind-LIDAR, optical backscatter, Doppler shift analysis, wave length ~ 1.5 µm ➔ wind and aerosol profiles

image:
Halo Photonics

SODAR

algorithms for the determination of mixing-layer height

and low-level jet observations

Institute for Meteorology and Climate Research – Atmospheric Environmental Research

monostatic SODAR: measuring principles

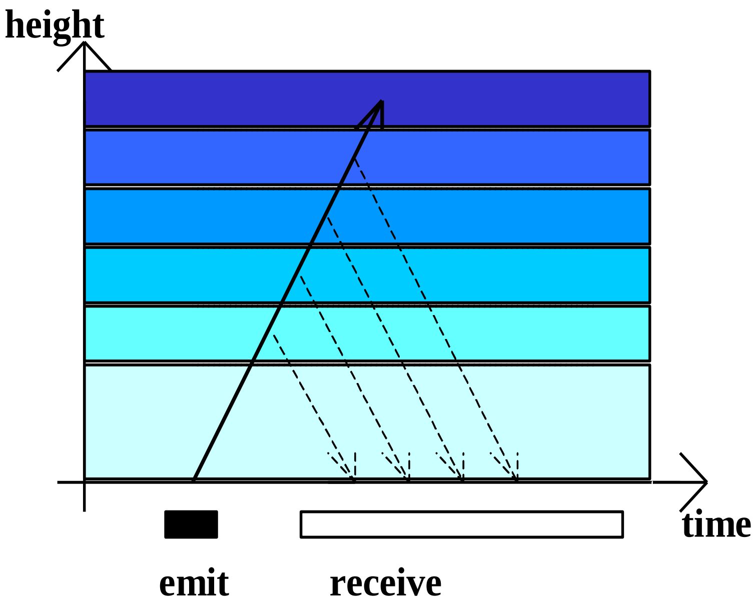

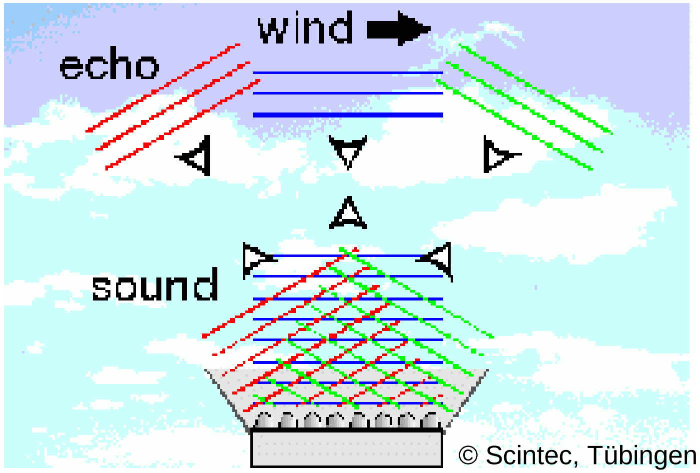

deduction:

sound travel time	=	height
backscatter intensity	=	turbulence
Doppler-shift	=	wind speed

Emission of sound waves into three directions:

in order to measure all three components of the wind (horizontal and vertical)

SODAR sample plot (daytime convective BL)

acoustic backscatter intensity

40 – 300 m

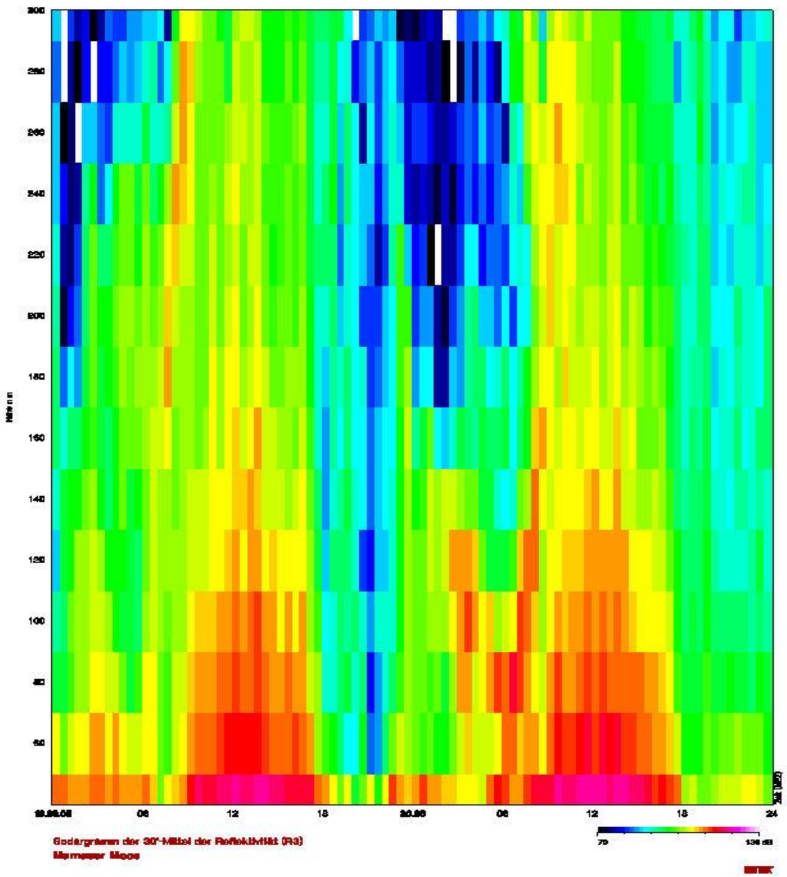

2 days, midnight to midnight

sigma w

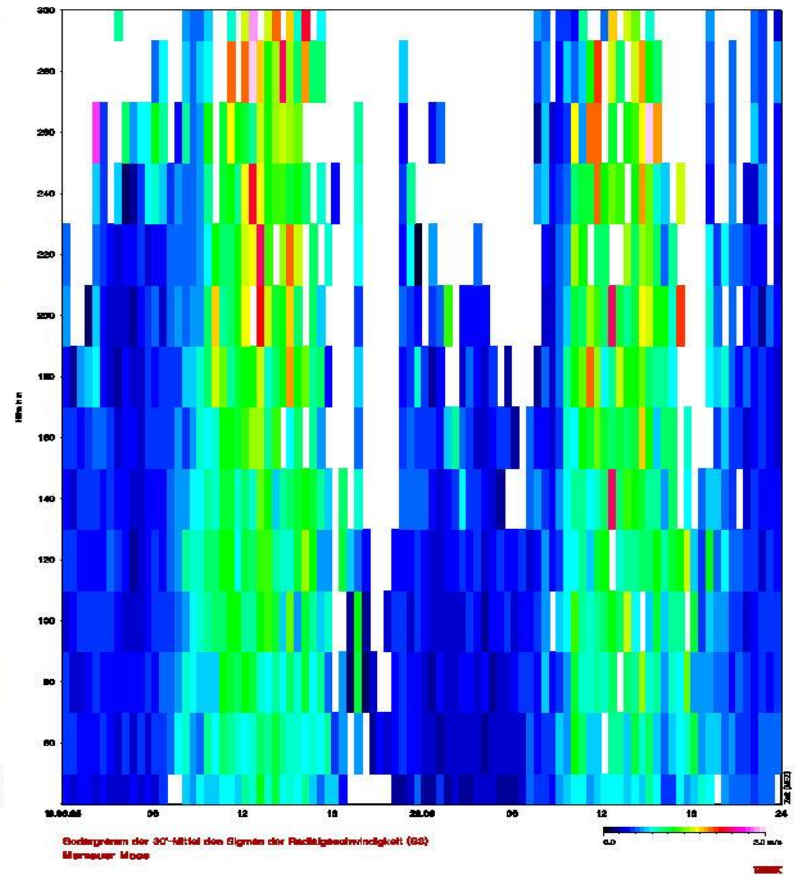

SODAR sample plot (lifted inversion)

acoustic backscatter intensity

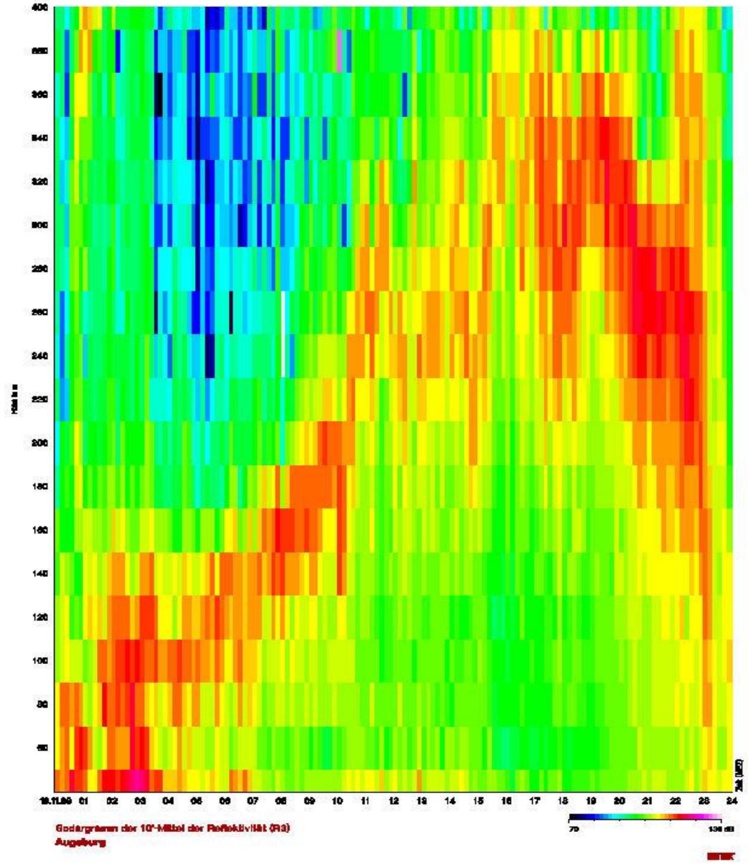

sigma w

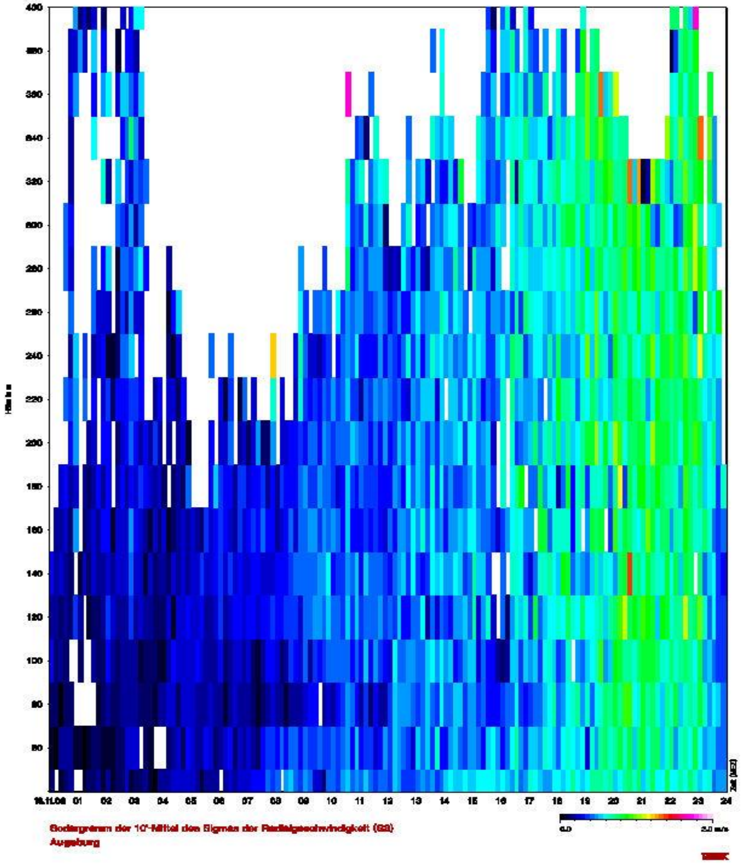

40 – 400 m

1 day, midnight to midnight

Algorithms to detect MLH from SODAR data

criterion 1:
upper edge of high turbulence

criterion 2:
surface and lifted inversions

MLH = Min (C1, C2)

Emeis, S., K. Schäfer, C. Münkel, 2008: Surface-based remote sensing of the mixing-layer height – a review. Meteorol. Z., **17**, 621-630.

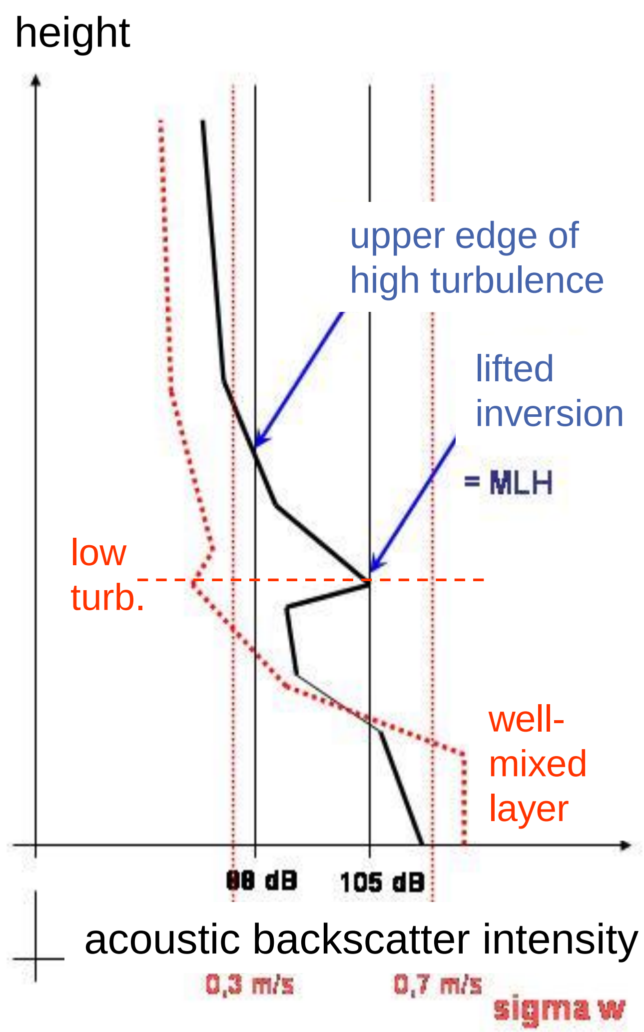

example 1: daytime

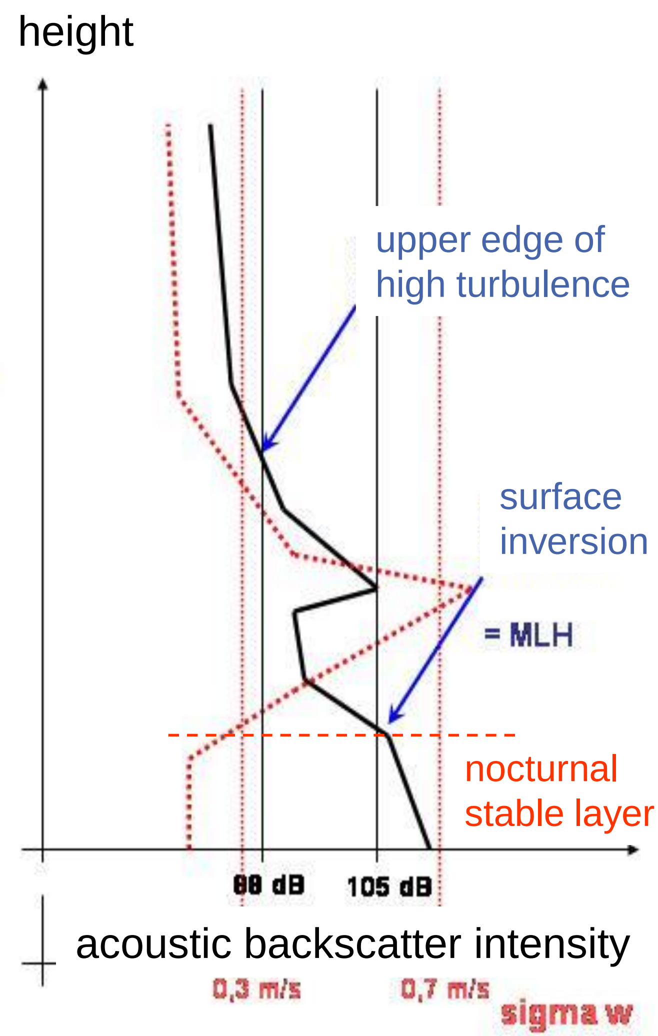

example 2: night-time

Eine unserer ersten großen SODAR-Messkampagnen

Karlsruhe Institute of Technology

	1 2002	1 2003
	2 2002	2 2003
	3 2002	3 2003
	4 2002	4 2003
5 2001	5 2002	
6 2001		
7 2001		
8 2001	8 2002	
9 2001	9 2002	
10 2001	10 2002	
11 2001	11 2002	
12 2001	12 2002	

AFO 2000

GEFÖRDERT VOM

Bundesministerium
für Bildung
und Forschung

METEK DSDR3x7-SODAR des IMK-IFU in Hannover-Linden

2-jährige Messperiode an ein und demselben Standort, davon 17 Monate mit demselben Mess-programm

Versuch einer analytischen Beschreibung des vertikalen Windprofils

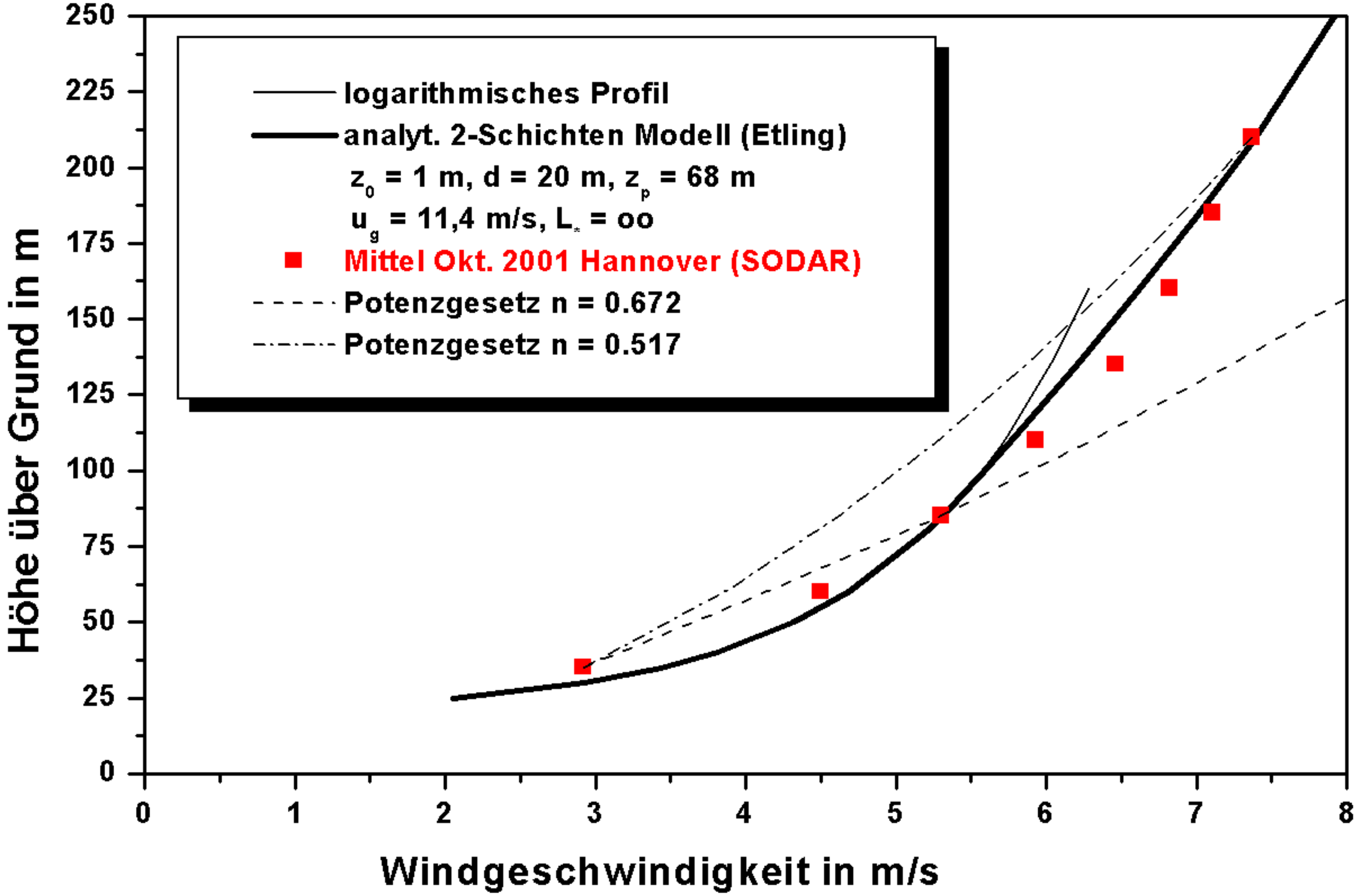

AFO 2000
GEFÖRDERT VOM
Bundesministerium für Bildung und Forschung

Ansätze für durchgehende Windprofilbeschreibung in der nicht neutral-geschichteten Grenzschicht (Emeis et al. 2007 basierend auf Etling 2002) mit der zusätzlichen Annahme, dass auch die vertikale Windscherung in der Höhe $z = z_p$ stetig ist:

$$u(z) = \begin{cases} u_* / \kappa\left(\ln(z/z_0) - \Psi_m(z/L_*)\right) & \text{for } z < z_p \\ u_g(-\sin\alpha_0 + \cos\alpha_0) & \text{for } z = z_p \\ u_g[1 - 2\sqrt{2}e^{-\gamma(z-z_p)} \sin\alpha_0 \cos(\gamma(z-z_p) + \pi/4 - \alpha_0) + 2e^{-2\gamma(z-z_p)} \sin^2\alpha_0]^{1/2} & \text{for } z > z_p \end{cases}$$

mit den externen Parametern z_0, L_* und u_g und den internen Parametern α_0, z_p und γ.

stefan.emeis@kit.edu
Institute for Meteorology and Climate Research – Atmospheric Environmental Research

mit den externen Parametern z_0 und u_g und den internen Parametern α_0, z_p und γ.

$$u_* = 2|u_g|\gamma\kappa z_p \sin\alpha_0$$

$$\alpha_0 = arctg \frac{1}{1 + 2\gamma z_p \ln(z_p / z_0)}$$

$$\gamma = \sqrt{\frac{f}{2\kappa u_* z_p}}$$

tagsüber

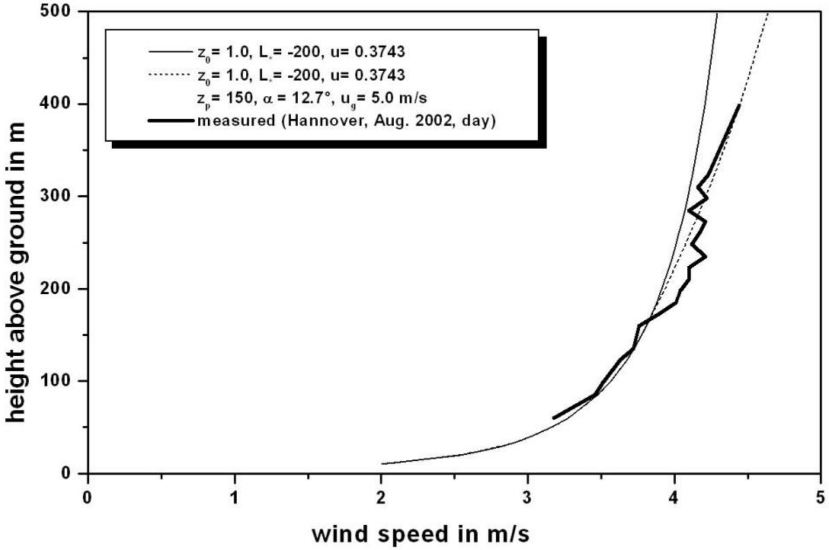

LLJ

nachts

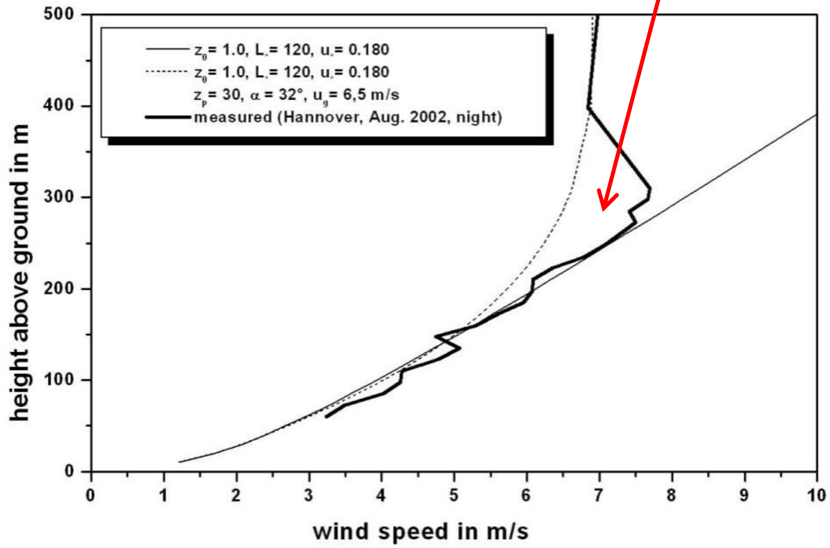

die gestrichelte Kurve zeigt die durchgehende Profilfunktion,
die durchgezogene Kurve ein nach oben fortgesetztes logarithmisches Profil

Mittlerer Tagesgang (Monatsmittel) der Inversionshöhe über Hannover

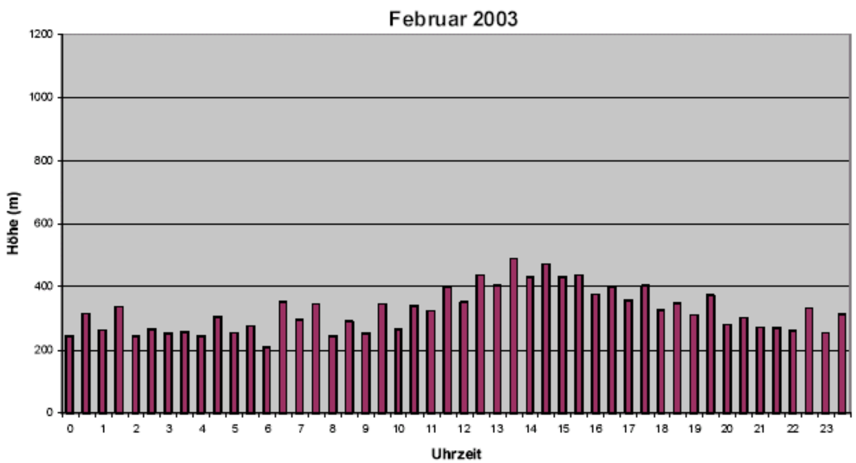

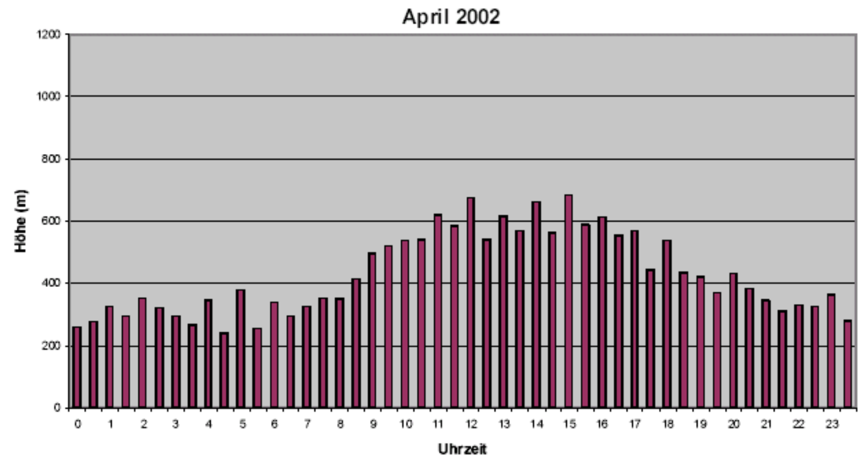

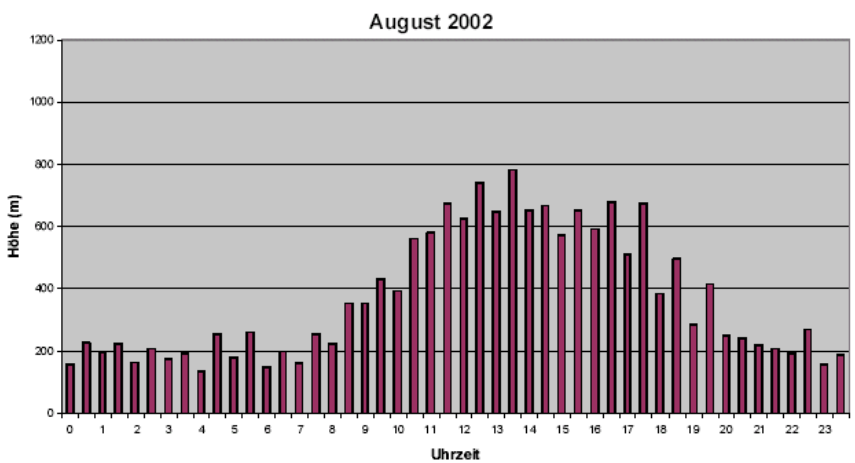

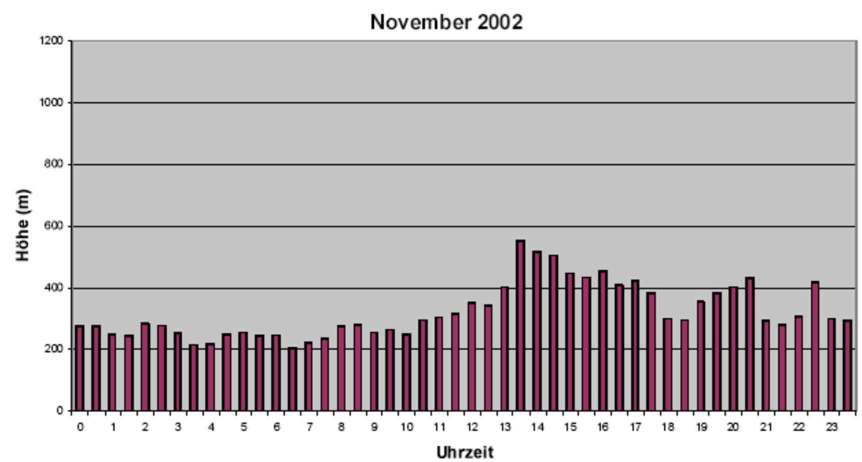

examples for low-level jet observations with SODAR

vertical profiles of wind speed (30 min means)

23-30 June 2005

AdP Ch d G

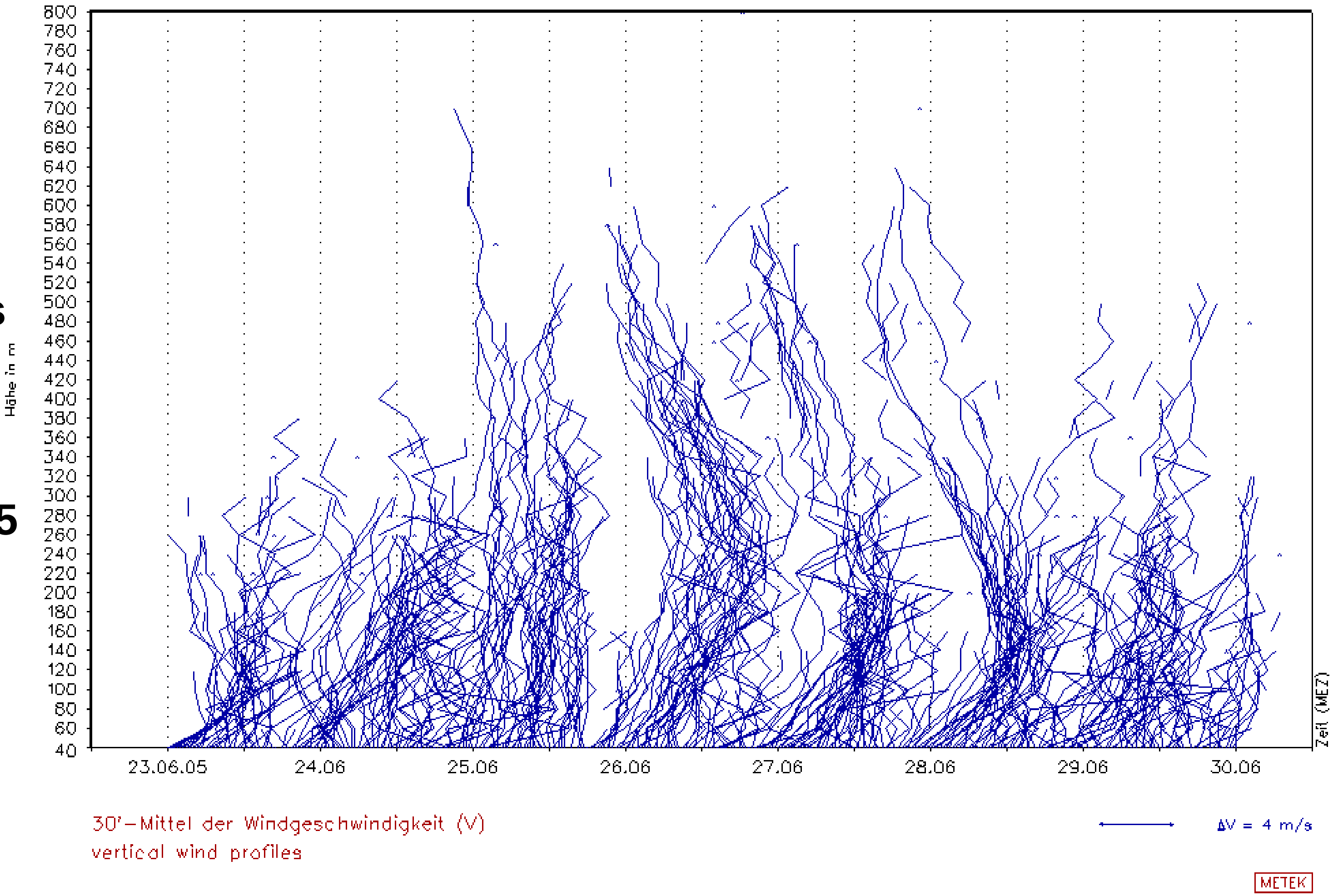

 stefan.emeis@kit.edu

Institute for Meteorology and Climate Research – Atmospheric Environmental Research

WindForS Wind Energy Research Alliance

KIT Karlsruhe Institute of Technology

Low-level jet

vertical profiles of wind speed

26 June 2005

AdP Ch d G

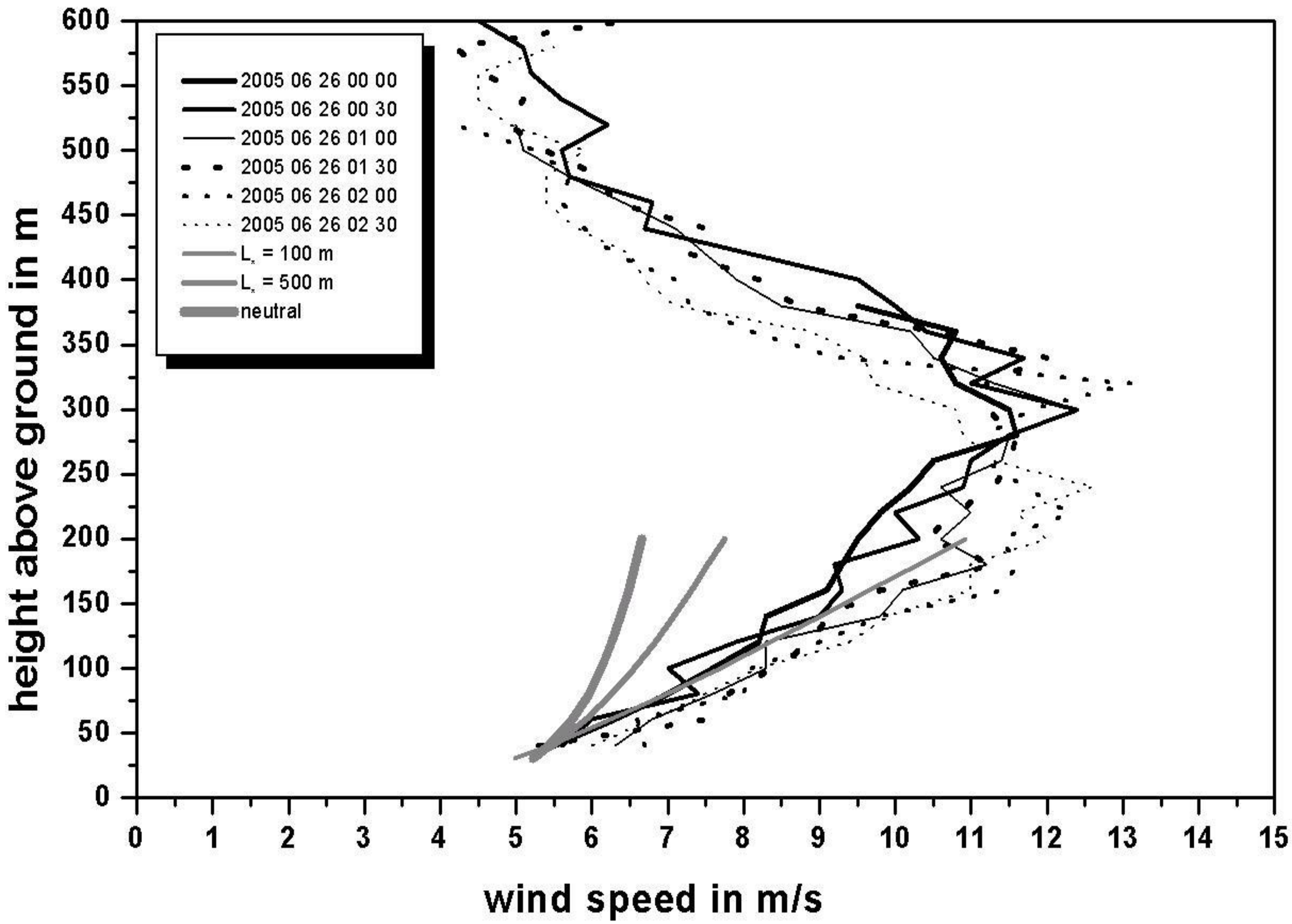

examples for low-level jet observations with SODAR

vertical profiles of wind direction

26 June 2005

AdP Ch d G

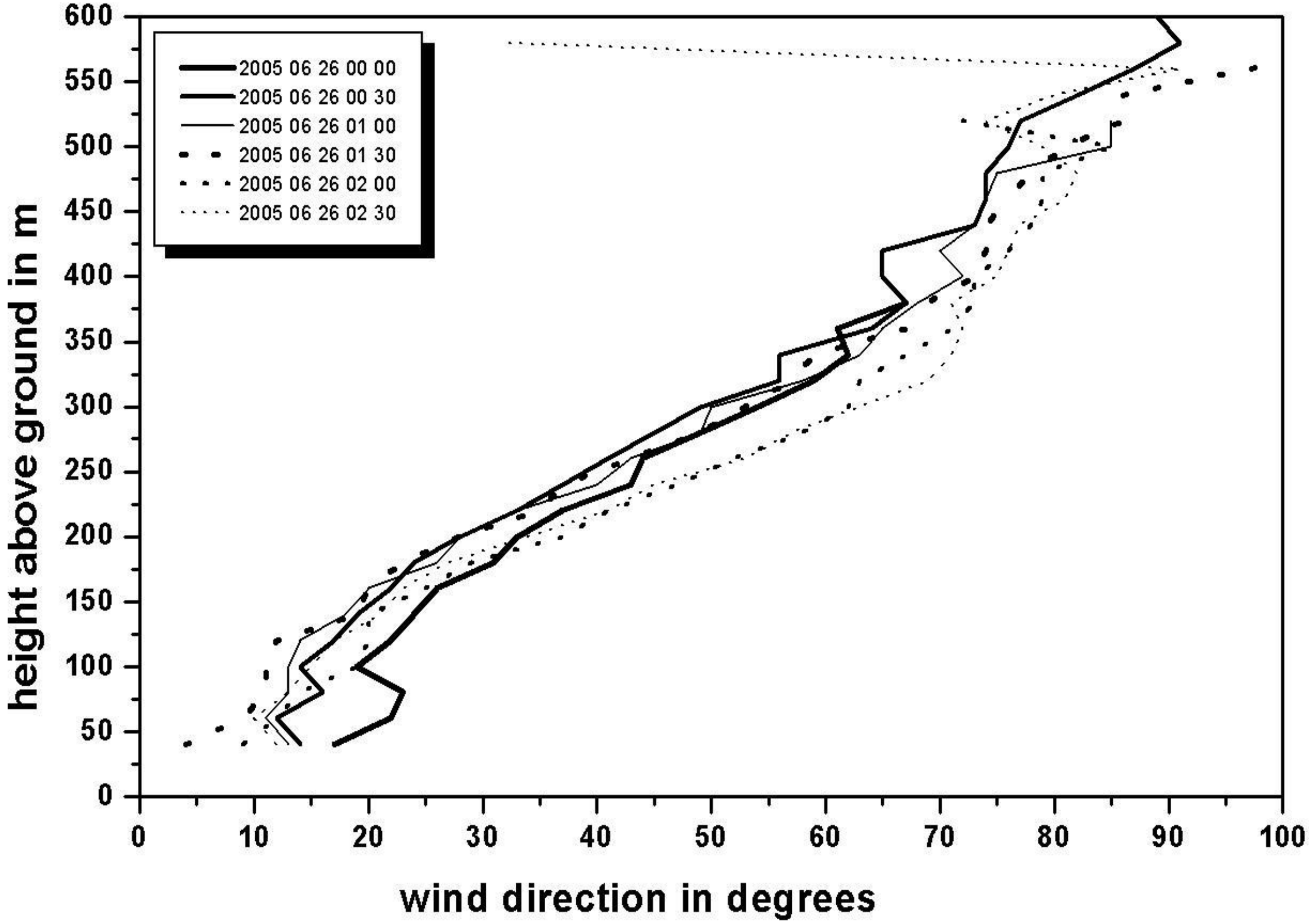

Institute for Meteorology and Climate Research – Atmospheric Environmental Research

Ceilometer

algorithms for the determination of mixing-layer height

Ceilometer/LIDAR measuring principle

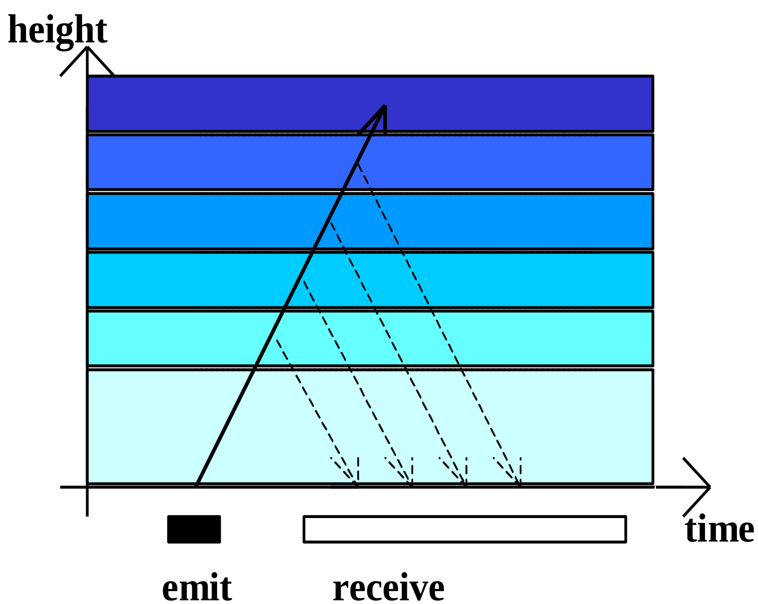

detection:

travel time of signal = height
backscatter intensity = particle size and number distribution
Doppler-shift = cannot be analyzed from ceilometer data
(available only from a Wind-LIDAR: velocity component in line of sight)

ceilometer sample plot (daytime convective BL)

optical backscatter intensity

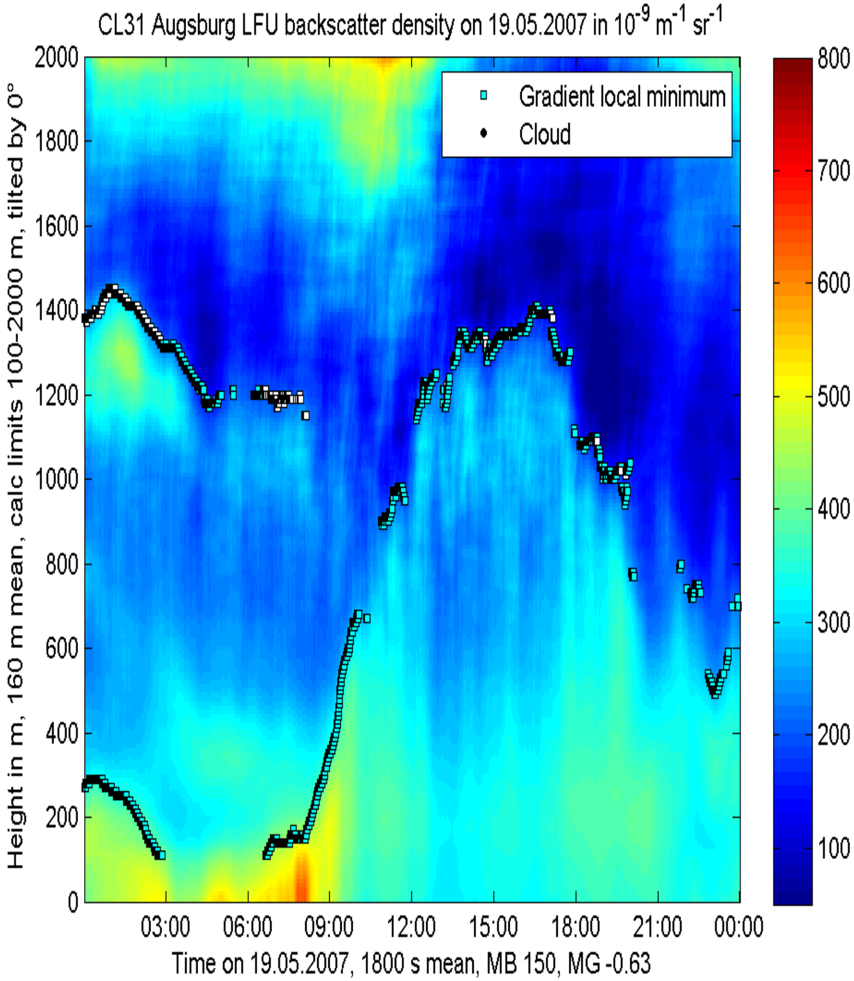

negative vertical gradient of optical backscatter intensity

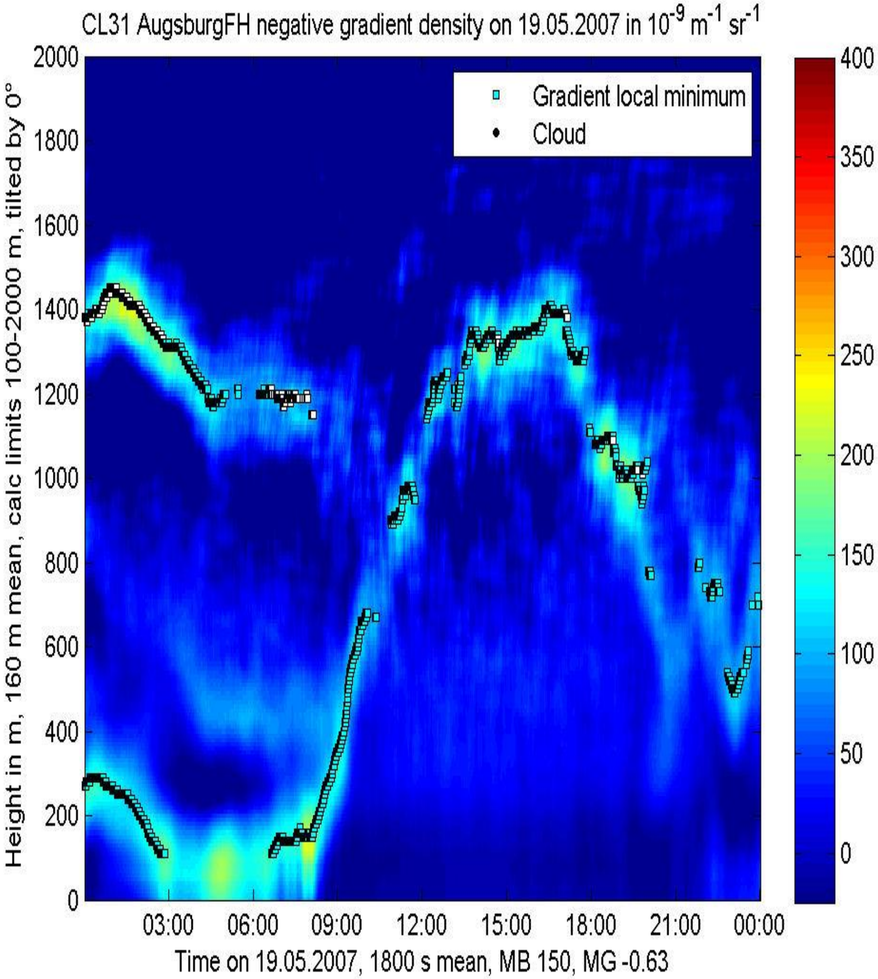

Algorithm to detect MLH from Ceilometer-Daten

criterion

minimal vertical gradient of backscatter intensity (the most negative gradient)

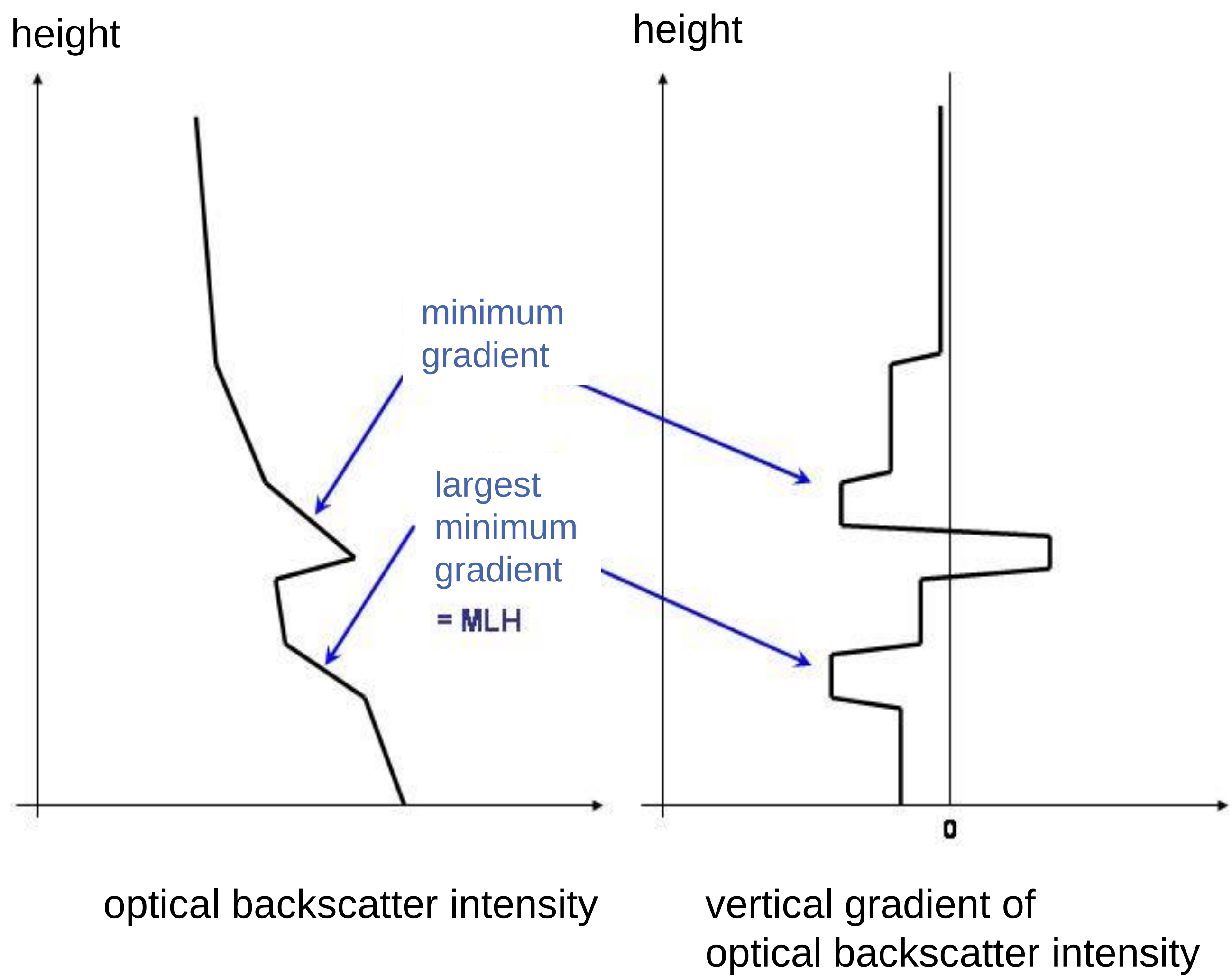

Different gradient methods (see Sicard et al. 2006, BLM 119, 135-157)

logarithmic gradient minimum

gradient minimum

inflection point method (minimum of 2nd derivative)

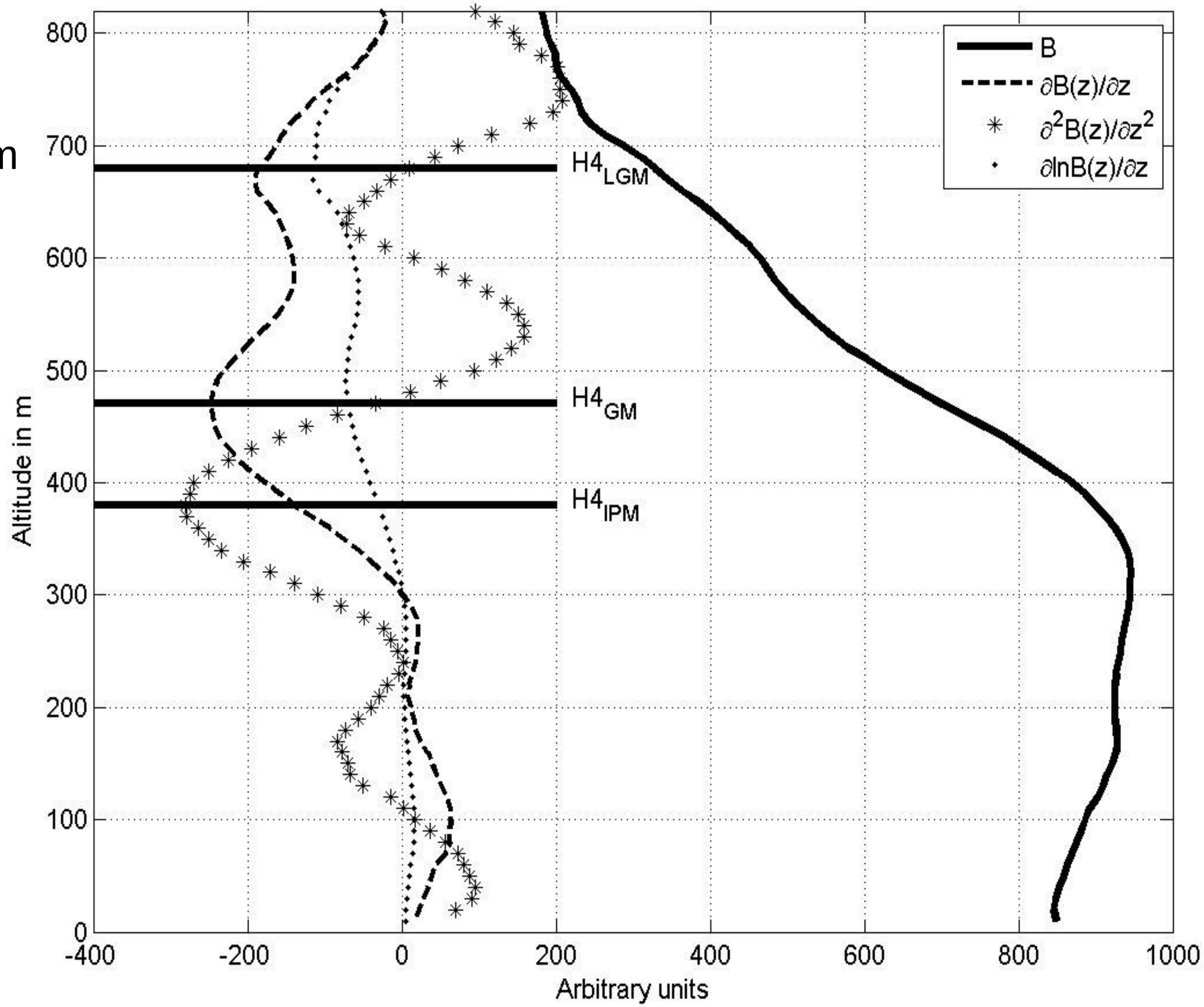

comparison of two different ceilometers

LD40

two optical axes
- wave length: 855 nm
- height resolution: 7.5 m
- max. range: 13000 m

CL31 / CL51

one optical axis
- wave length: 905 nm
- height resolution: 5 m
- max. range: 7500 m

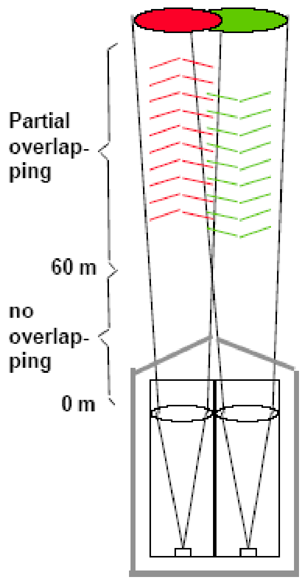

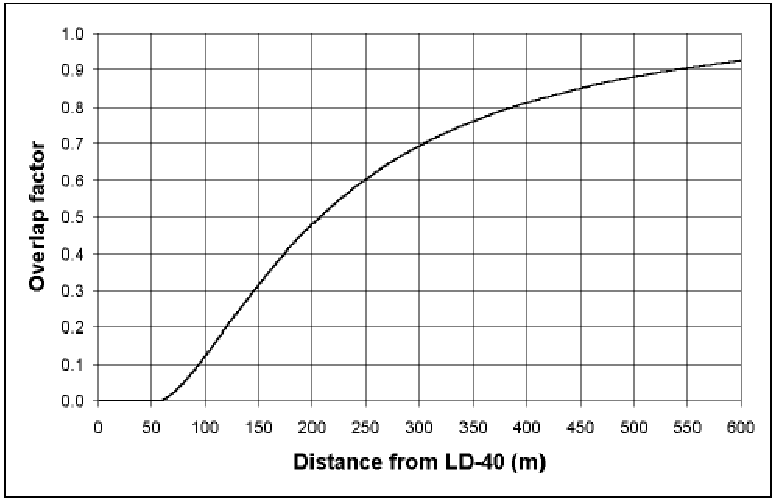

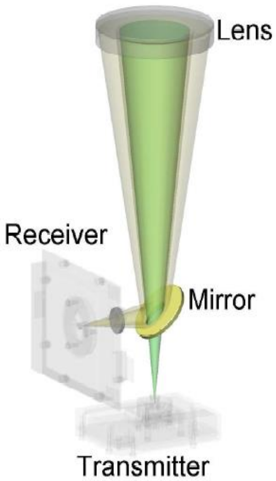

comparison of LD40 and CL31

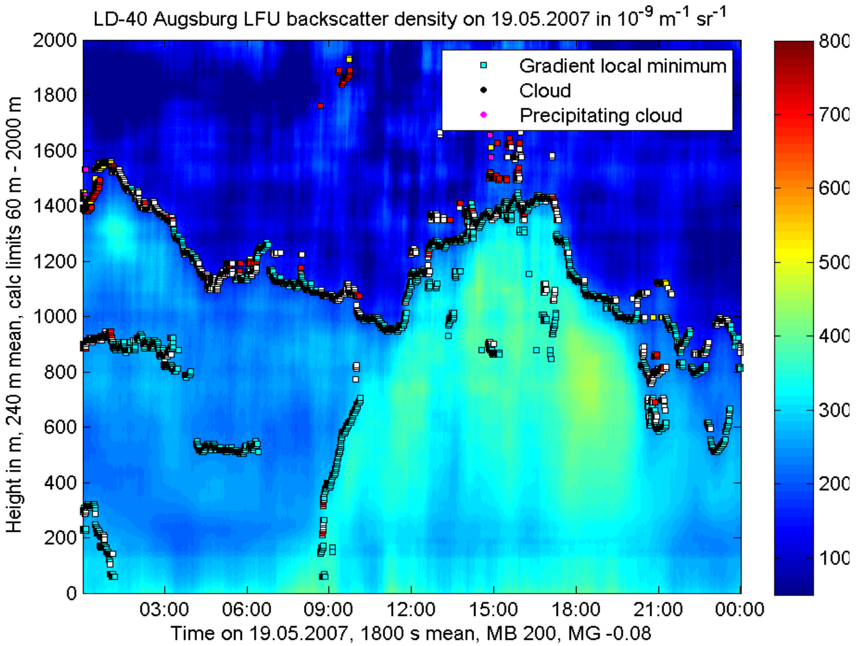

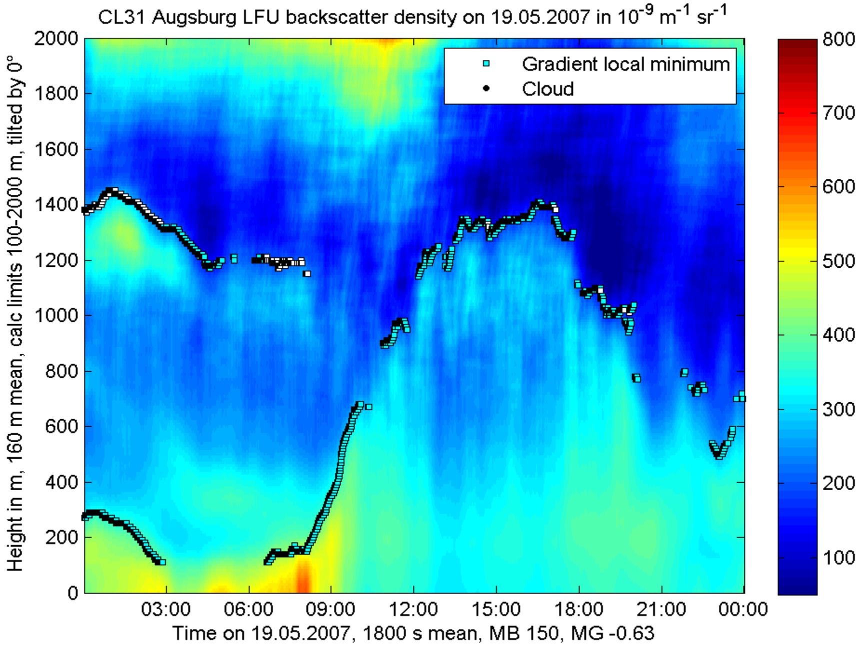

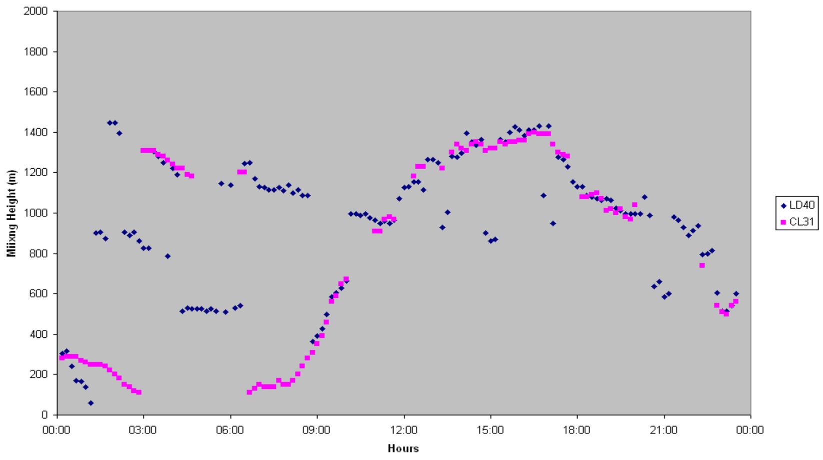

Eyjafjallajökull ash cloud over Southern Germany

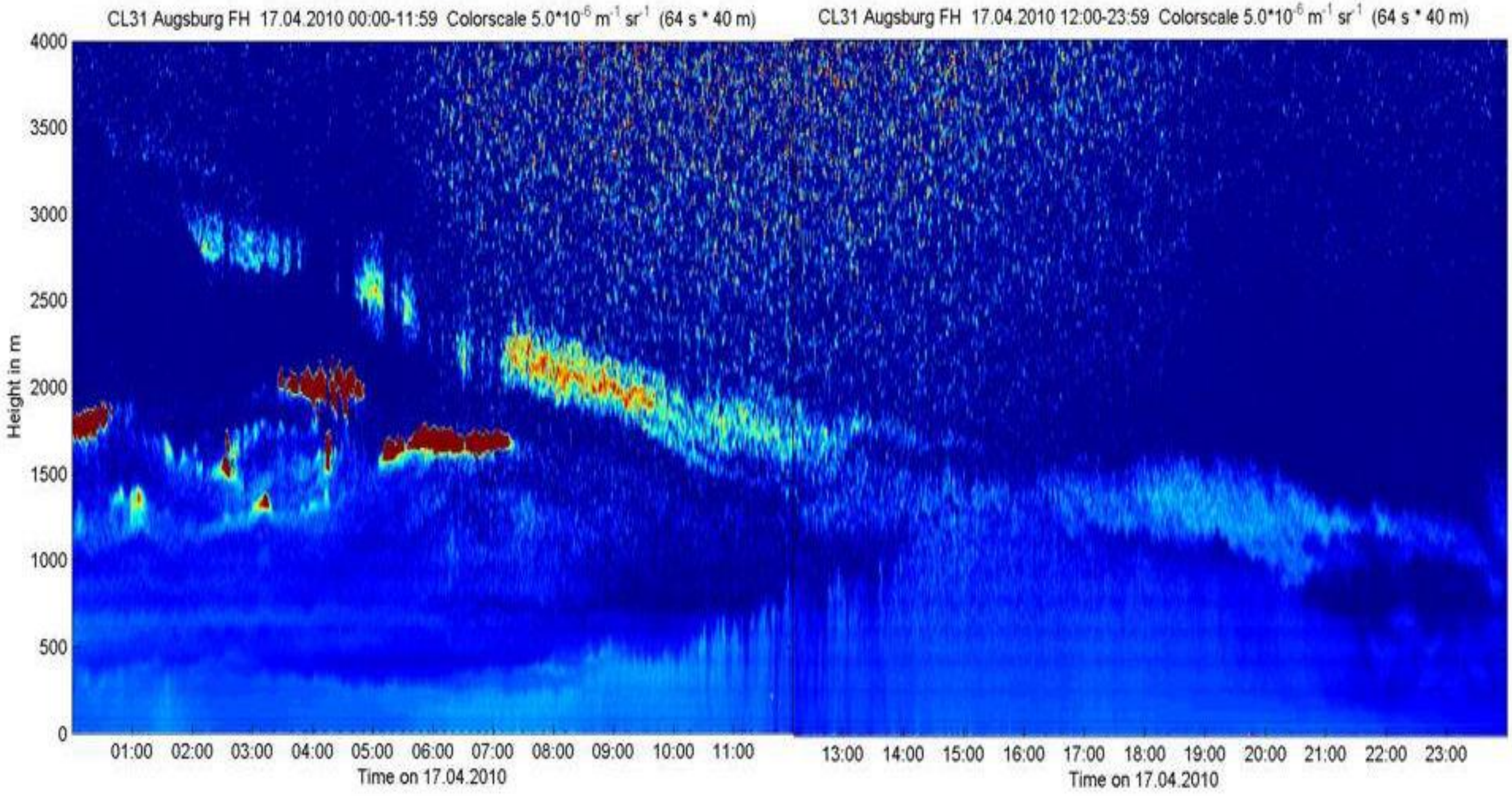

read more: Emeis, S., R. Forkel, W. Junkermann, K. Schäfer, H. Flentje, S. Gilge, W. Fricke, M. Wiegner, V. Freudenthaler, S. Groß, L. Ries, F. Meinhardt, W. Birmili, C. Münkel, F. Obleitner, P. Suppan, 2011: Measurement and simulation of the 16/17 April 2010 Eyjafjallajökull volcanic ash layer dispersion in the northern Alpine region. Atmos. Chem. Phys., 11, 2689–2701

RASS

principles of operation

examples

RASS measuring principle

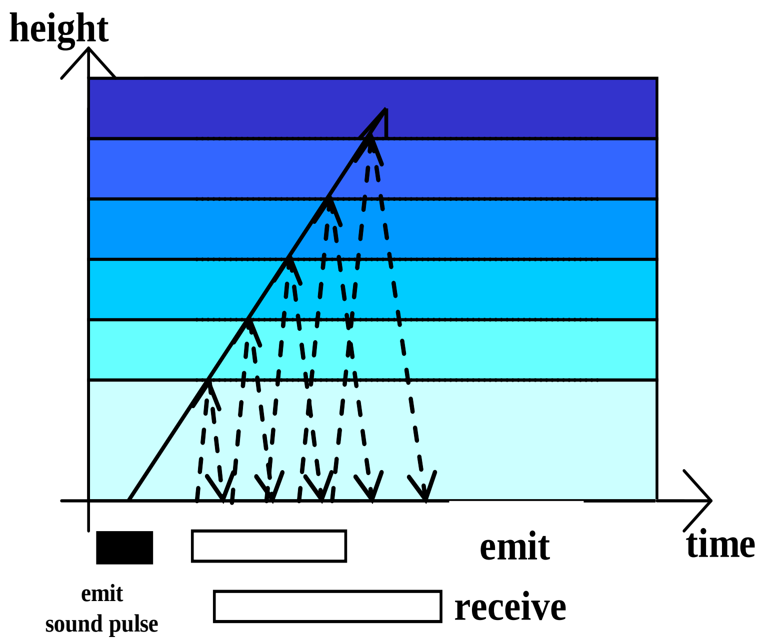

detection:

travel time of em./ac. signal = height
ac. backscatter intensity = turbulence (identical to SODAR)
ac. Doppler-shift = line-of-sight wind speed (identical to SODAR)
em. Doppler shift = sound speed ➔ temperature

RASS: frequencies

Bragg condition:
acoustic wavelength = ½ electro-magnetic wavelength

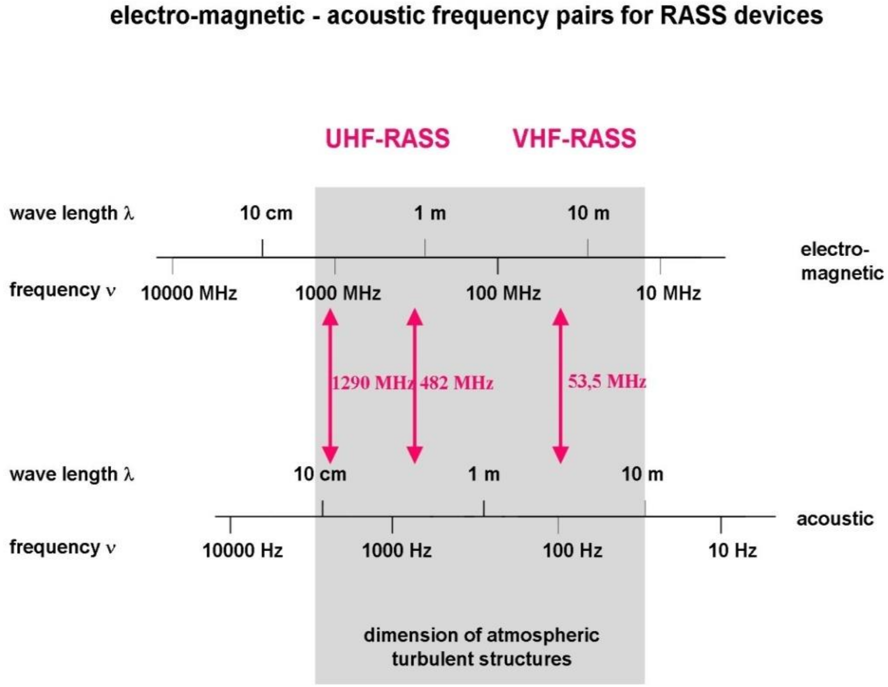

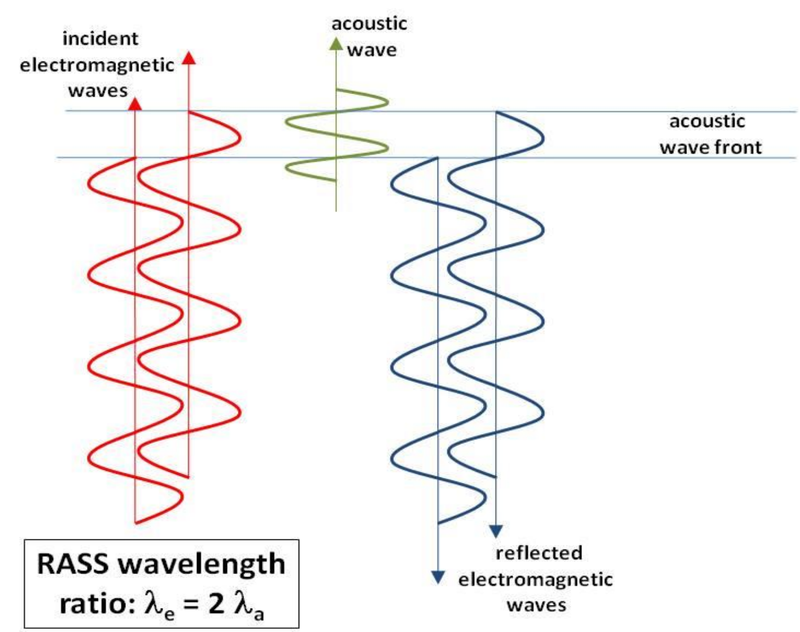

Emeis, S., 2010: Measurement Methods in Atmospheric Sciences - In situ and remote. Borntraeger, Stuttgart, 272 pp., 103 figs, 28 tables, ISBN 978-3-443-01066-9.

SODAR-RASS
(Doppler-RASS)

(METEK)

acoustic frequ.: 1077 Hz
radio frequ.: 474 MHz
resolution: 20 m
lowest
range gate: ca. 40 m

vertical range: 540 m

example RASS data: summer day
potential temperature (left), horizontal wind (right)

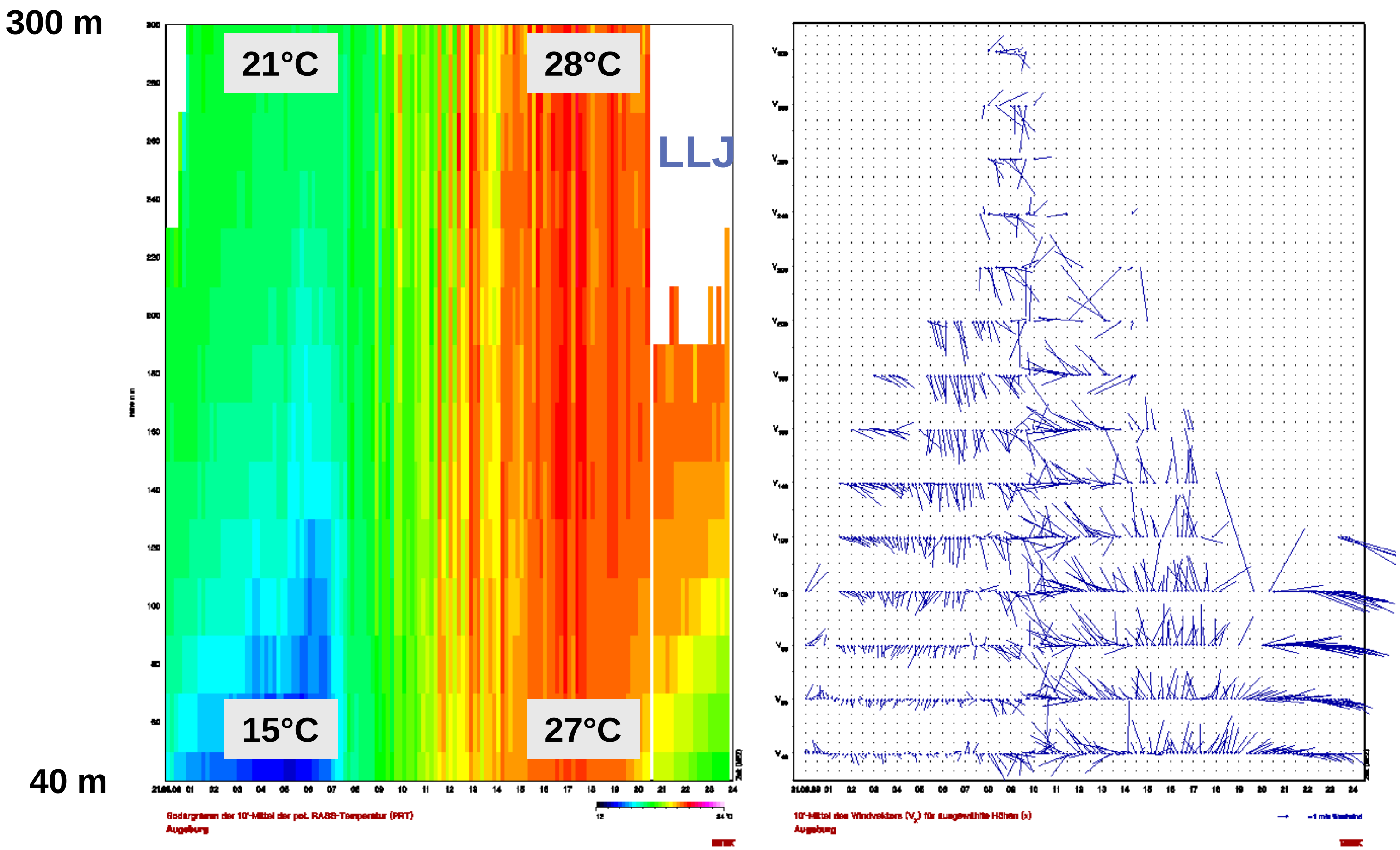

example RASS data: winter day

potential temperature (left), horizontal wind (right)

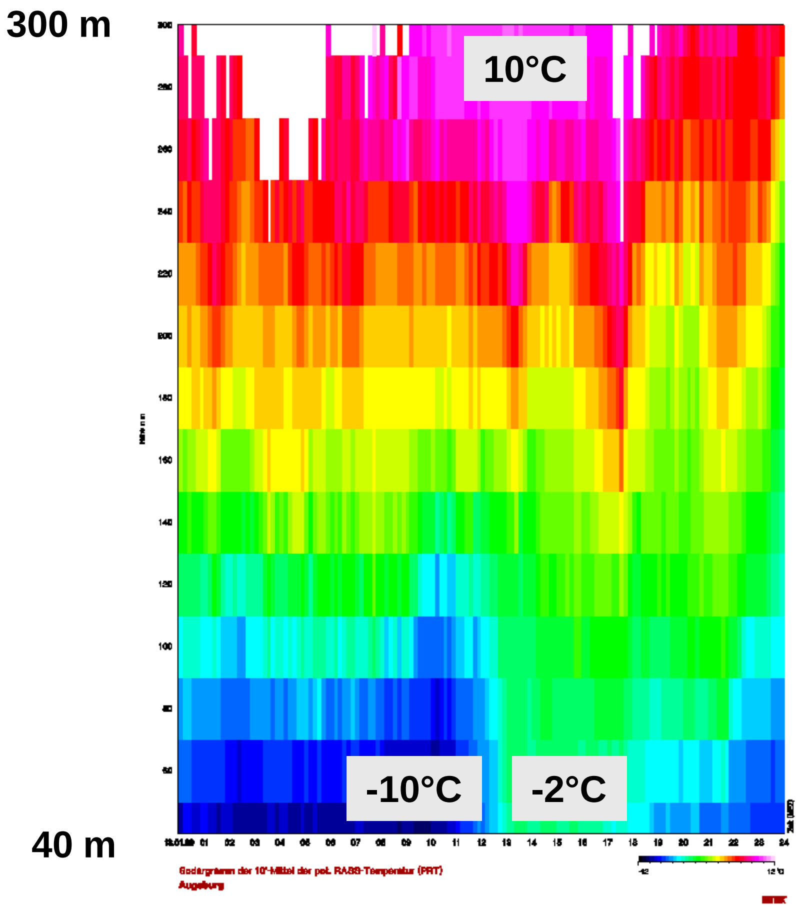

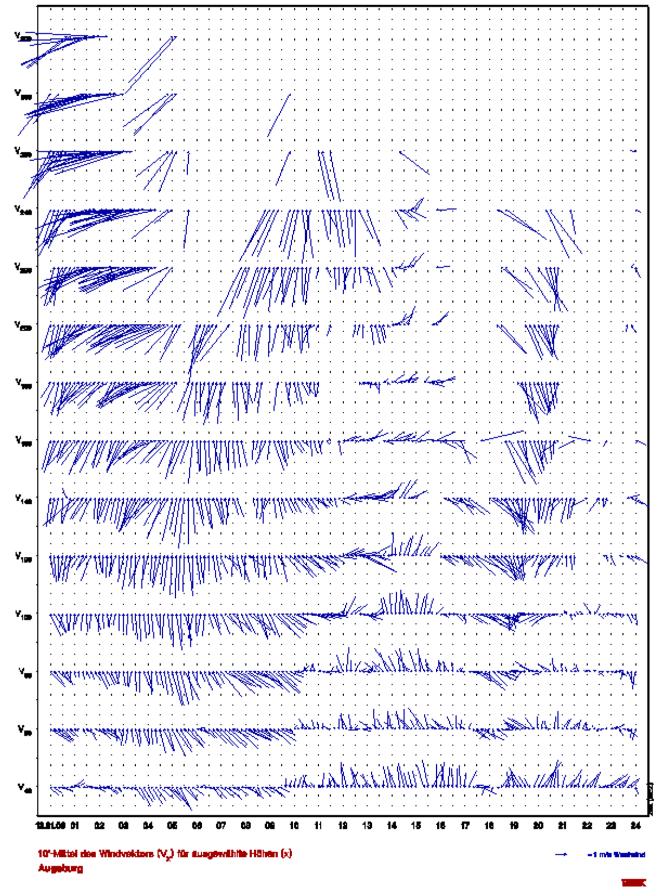

Doppler windlidar

wind, turbulence, aerosol detection, mixing-layer height, low-level jet

Doppler windlidar measuring principle

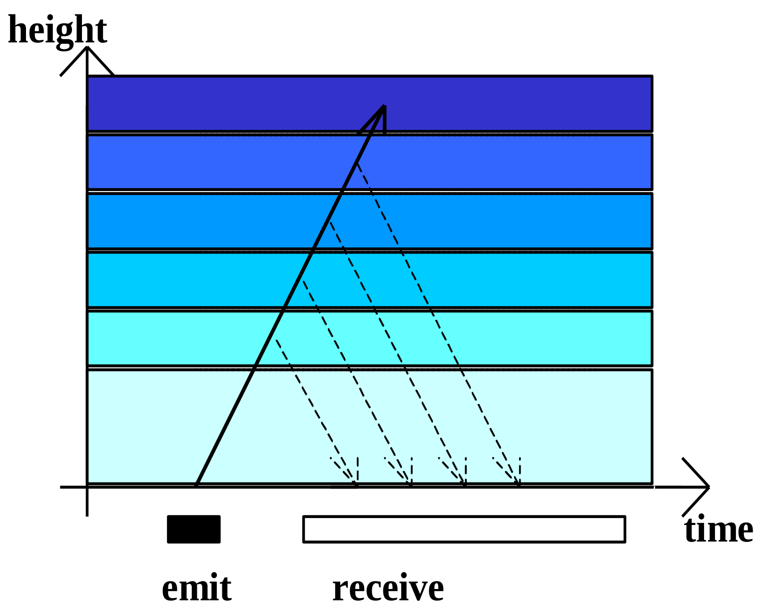

detection:

travel time of signal = height
backscatter intensity = particle size and number distribution
depolarisation = particle shape
Doppler-shift = wind speed in the line of sight

mobile Doppler windlidar from Halo Photonics

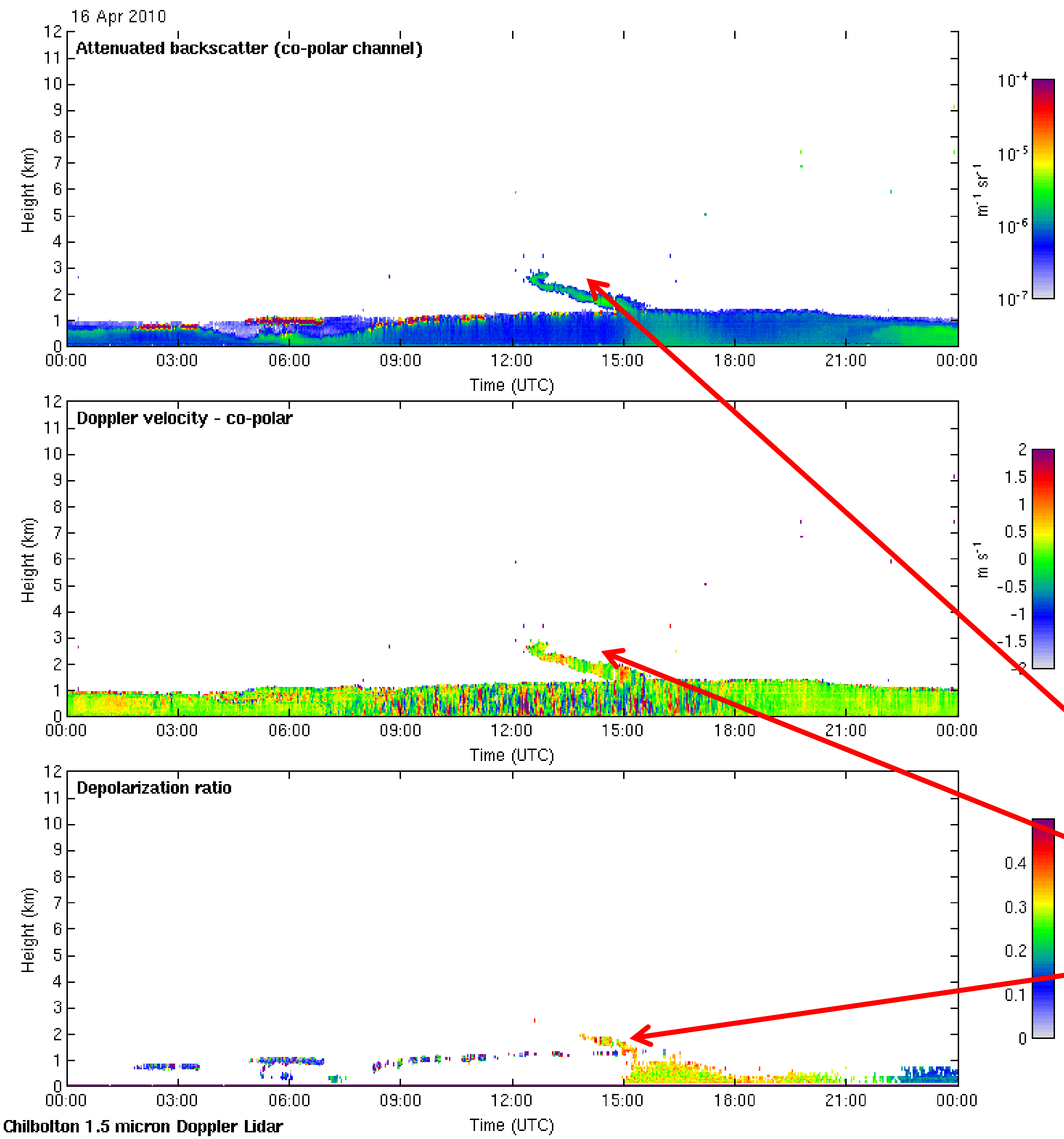

sample data from windlidar

April 16, 2010

by
Univ. of Reading

taken at

Chilbolton, UK

http://www.met.reading.ac.uk/radar/realtime/archive/doppler-lidar/20100416_chilbolton_halo-doppler-lidar.png

volcanic ash from Eyjafjallajokull

realtime data: http://www.chilbolton.rl.ac.uk/weather/lidar.htm

WINDFORS Wind Energy Research Alliance

KIT Karlsruhe Institute of Technology

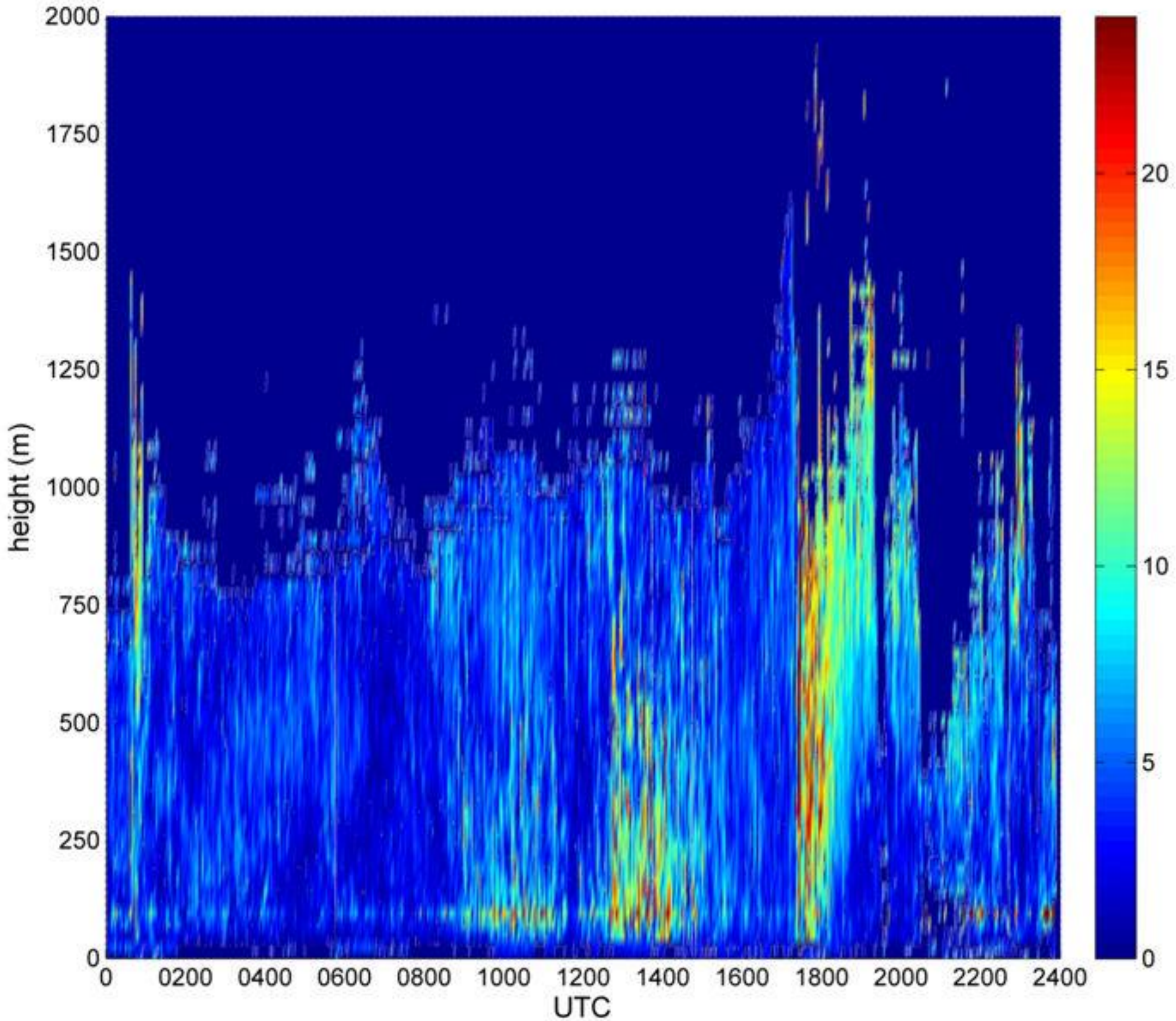

sample data from windlidar

wind speeds in m/s (colour bar)

June 22, 2011

by IMK-IFU

taken at

Garmisch-Partenk., Germany

Comparisons between different instruments

temperature profile and aerosol backscatter

comparison of RASS data (potential temperature, right) with aerosol backscatter from a ceilometer (left)

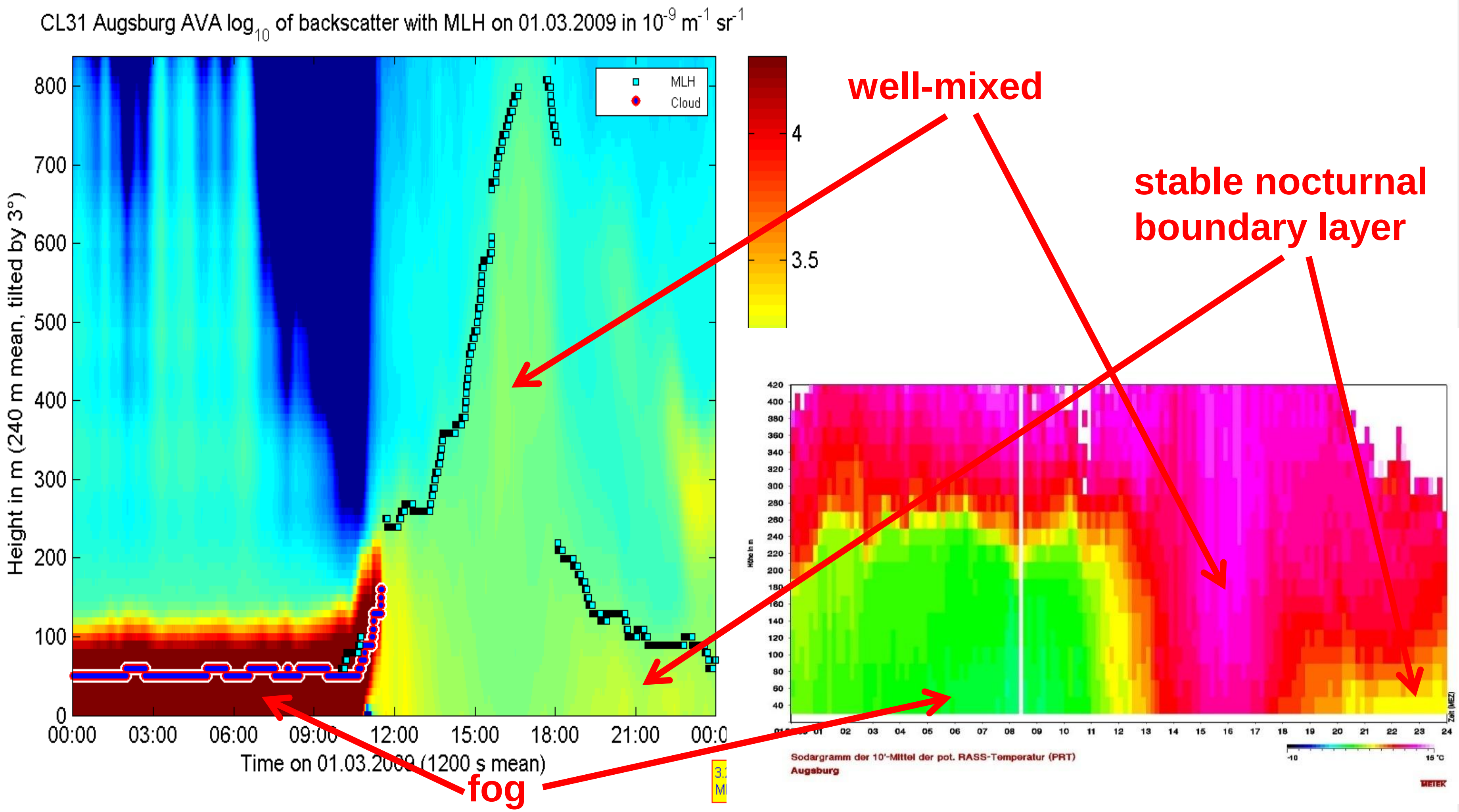

Detection of the diurnal variation of PBL structure from SODAR and Ceilometer data taken in Budapest

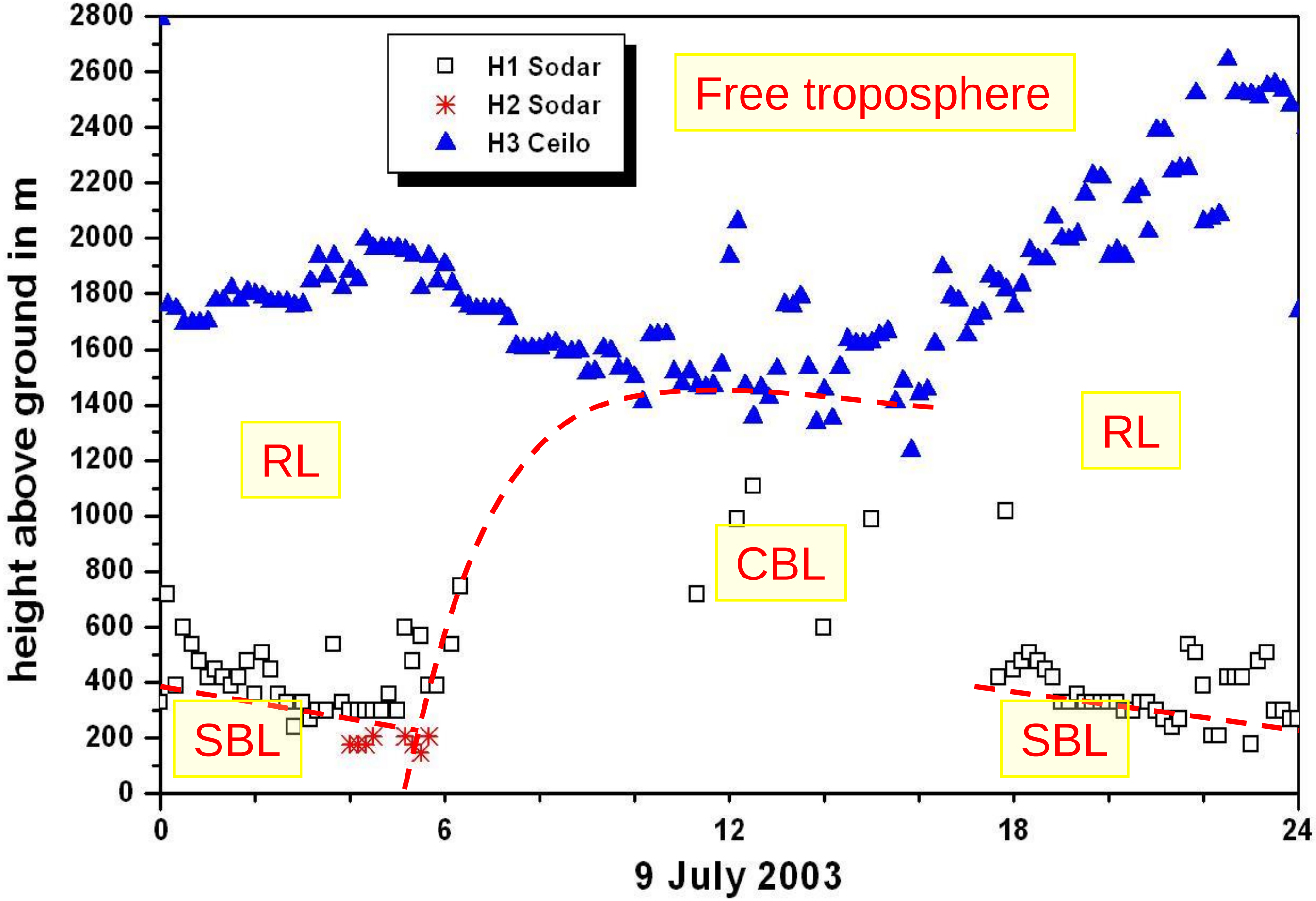

SBL:

stable boundary layer (usually at night and in winter)

CBL:

convective boundary layer (usually at daytime due to strong insolation)

RL:

residual layer (usually at night-time)

Emeis, S., K. Schäfer, 2006: Remote sensing methods to investigate boundary-layer structures relevant to air pollution in cities. Bound.-Lay Meteorol., 121, 377-385,

Comparison of MLH retrievals with three different remote sensing techniques

SODAR
acoustic backscatter

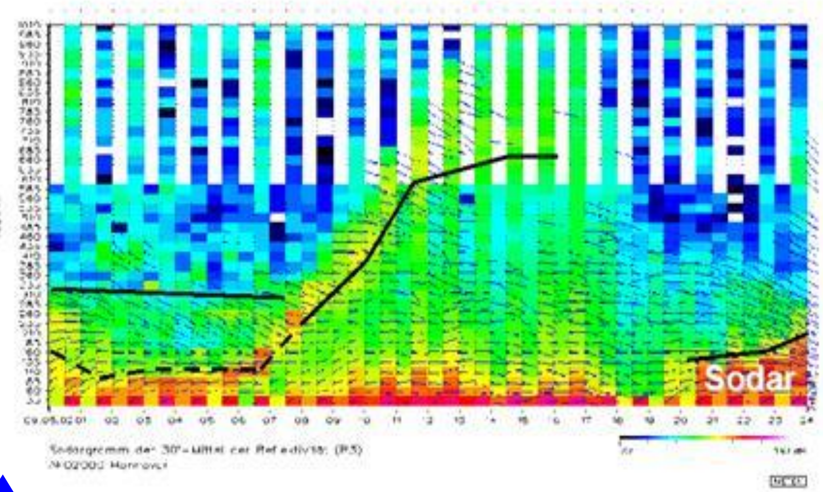

ceilometer
optical backscatter

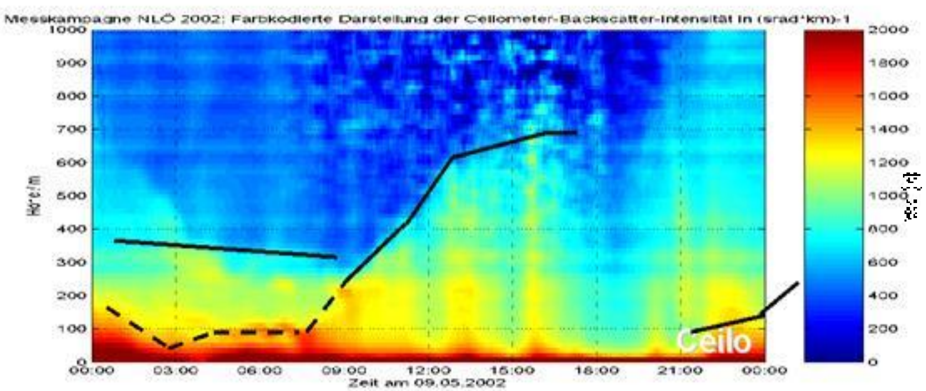

RASS
temperature

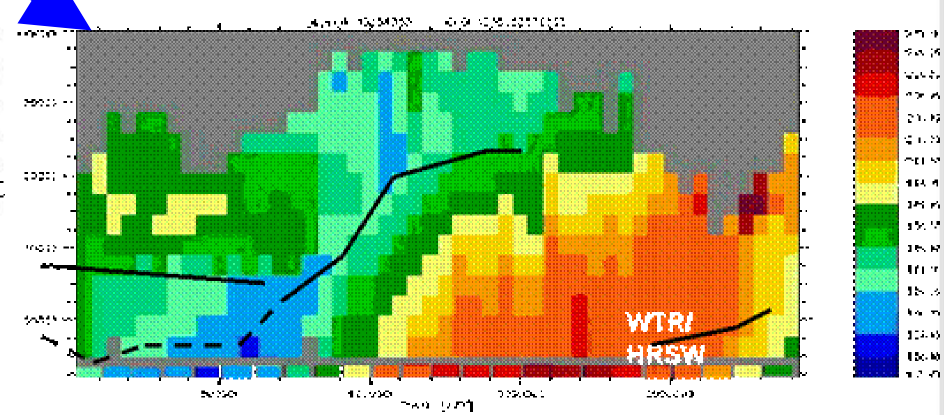

Emeis, S., Chr. Münkel, S. Vogt, W.J. Müller, K. Schäfer, 2004: Atmospheric boundary-layer structure from simultaneous SODAR, RASS, and ceilometer measurements. Atmos. Environ., 38, 273-286.

Application of MLH information for regional emission flux estimates

Determination of regional surface emission fluxes of a substance e

Assumptions:

- horizontal homogeneity
- no fluxes through the upper boundary (inversion)
- no sources and sinks within the volume of interest

$$\int_{S_{surf}} \overline{e'w'} \cdot dS = \int_V \frac{de}{dt} dV$$

simultaneous measurement of concentration and MLH

(inverse method)

c_{CH4}

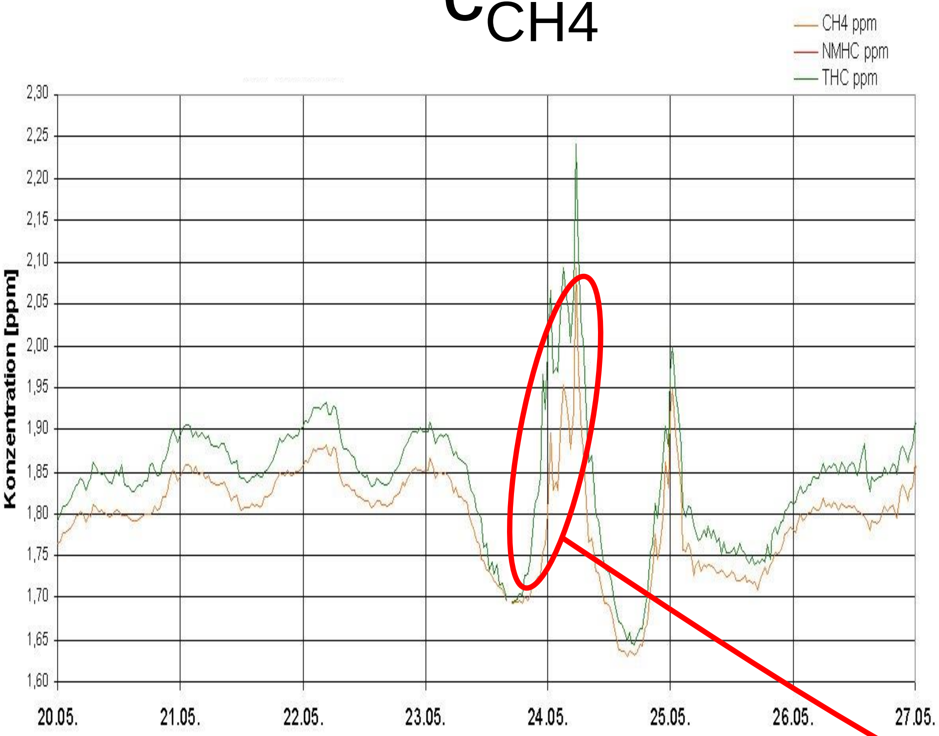

MLH

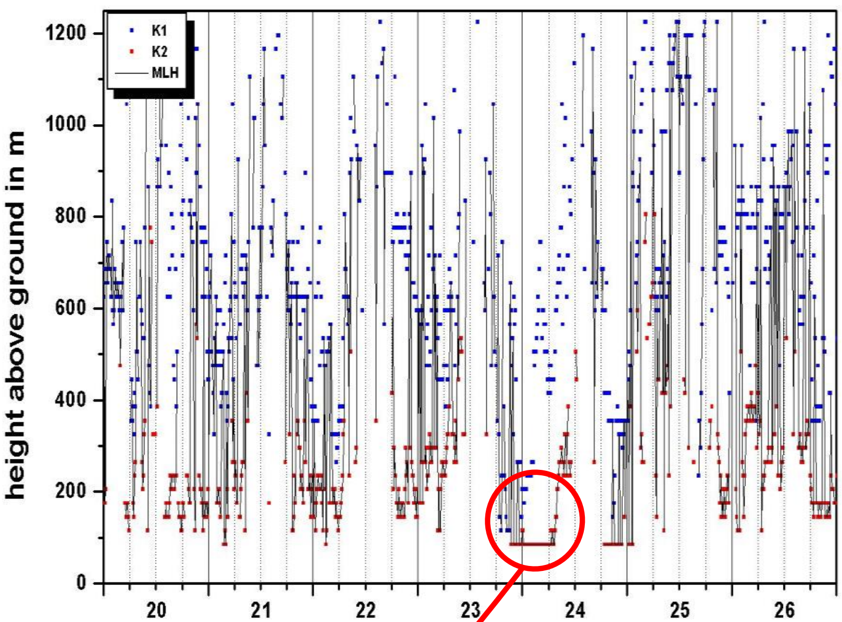

20.-26.05.2003

determination of regional $[C_{CH4}{}'w']_{surf}$ (curves) from concentration changes (x-axis) and MLH (y-axis)

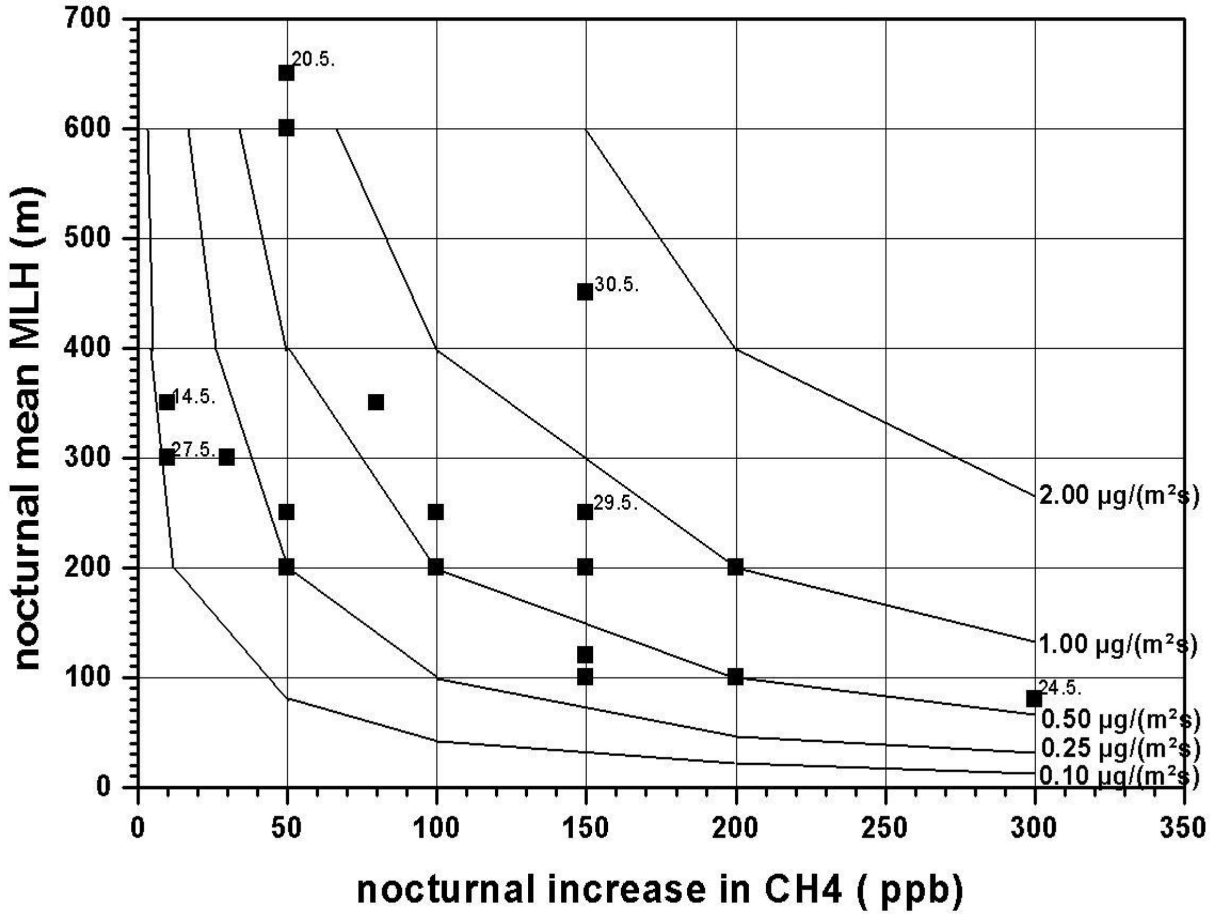

determination of regional $[C_{CH4}'w']_{surf}$ (curves) from concentration changes and remotely sensed MLH

methane emissions:

typical values obtained here:

span:	0.10 to 2.00 µg/(m² s)
mean value:	0.50 µg/(m² s)

average values from national reporting (Kyoto protocol):

for entire Germany:	0.20 µg/(m² s)
among this from agriculture:	0.13 µg/(m² s)

Summary

☺ ☺ ☺ 💣 **RASS delivers temperature profiles, wind profiles are additionally available.**
MLH directly from temperature profiles. LLJ from wind profiles.
Does not work properly under high wind speeds. Restricted range.

☺ ☺ ☺ 💣 **wind lidar detects wind profiles, aerosol distribution and water droplets.**
It has to be assumed that the aerosol follows the thermal structure of the atmosphere and the wind.
MLH from aerosol backscatter, wind speed variance, LLJ from wind profiles.
Does not work properly in extreme clear (aerosol-free) air and during precipitation events and fog.

☺ ☺ 💣💣 **Ceilometer detects aerosol distribution and water droplets. It has to be assumed that the aerosol follows the thermal structure of the atmosphere.**
MLH indirectly from aerosol backscatter using a MLH algorithm.
Does not work properly in extreme clear (aerosol-free) air and during precipitation events and fog.

☺ 💣💣💣 **SODAR detects wind profiles, temperature fluctuations and gradients, but no absolute temperature.**
MLH indirectly from acoustic backscatter (MLH algorithm). LLJ from wind profiles.
Does not work properly under perfectly neutral stratification, with very high wind speeds, and during stronger precipitation events. Restricted range.

Literature

SODAR:

Asimakopoulos, D.N., C.G. Helmis, J. Michopoulos, 2004: Evaluation of SODAR methods for the determination of the atmospheric boundary layer mixing height. - Meteor. Atmos. Phys. 85, 85–92.

Beyrich, F., 1997: Mixing height estimation from sodar data – a critical discussion. - Atmos. Environ. 31, 3941–3953.

Ceilometer:

Schäfer, K., S.M. Emeis, A. Rauch, C. Münkel, S. Vogt, 2004: Determination of mixing-layer heights from ceilometer data. In: Remote Sensing of Clouds and the Atmosphere IX. Schäfer, K., A. Comeron, M. Carleer, R.H. Picard, N. Sifakis (Eds.), Proc. SPIE, Bellingham, WA, USA, Vol. 5571, 248–259.

Sicard, M., C. Pérez, F. Rocadenbosch, J.M. Baldasano, D. García-Vizcaino, 2006: Mixed-Layer Depth Determination in the Barcelona Coastal Area From Regular Lidar Measurements: Methods, Results and Limitations. - Bound.-Lay. Meteor. 119, 135–157.

RASS:

Engelbart, D.A.M., J. Bange, 2002: Determination of boundary-layer parameters using wind profiler/RASS and sodar/RASS in the frame of the LITFASS project. Theor. Appl. Climatol. 73, 53–65.

Emeis, S., K. Schäfer, C. Münkel, 2009: Observation of the structure of the urban boundary layer with different ceilometers and validation by RASS data. Meteorol. Z., 18, 149-154. (Open access, freely available from http://dx.doi.org/10.1127/0941-2948/2009/0365)

Emeis, S., K. Schäfer, C. Münkel, R. Friedl, P. Suppan, 2011: Evaluation of the interpretation of ceilometer data with RASS and radiosonde data. Bound.-Lay. Meteorol., online April 5, 2011. DOI: 10.1007/s10546-011-9604-6

Windlidar:

Emeis, S., M. Harris, R.M. Banta, 2007: Boundary-layer anemometry by optical remote sensing for wind energy applications. - Meteorol. Z., 16, 337-347.

Reginal budget studies:

Emeis, S., 2008: Examples for the determination of turbulent (sub-synoptic) fluxes with inverse methods. Meteorol. Z., 17, 3-11. DOI: 10.1127/0941-2948/2008/0265

Reviews:

Emeis, S., K. Schäfer, C. Münkel, 2008: Surface-based remote sensing of the mixing-layer height – a review. - Meteorol. Z., 17, 621-630. (Open access, freely available from http://dx.doi.org/10.1127/0941-2948/2008/0312)

Books:

wind energy meteorology:

Emeis, S., 2012: Wind Energy meteorology. Series: Green Energy and Technology. Springer Heidelberg etc., XIV+196 pp. H/C. ISBN: 978-3-642-30522-1, DOI: 10.1007/978-3-642-30523-8

boundary-layer remote sensing with application examples:

Emeis, S., 2011: Surface-Based Remote Sensing of the Atmospheric Boundary Layer. Series: Atmospheric and Oceanographic Sciences Library, Vol. 40. Springer Heidelberg etc., X+174 pp. 114 illus., 57 in color., H/C. ISBN: 978-90-481-9339-4, DOI: 10.1007/978-90-481-9340-0

overview on the entire range of meteorological measurement methods:

Emeis, S., 2010: Measurement Methods in Atmospheric Sciences. In situ and remote. Series: Quantifying the Environment Vol. 1. Borntraeger Stuttgart. XIV+257 pp., 103 Figs, 28 Tab. ISBN 978-3-443-01066-9.

Karlsruhe Institute of Technology

Thank you very much for your attention